Midpoint Report
Thermodynamic Demonstration Unit

October 19, 2018

Team 1A
Jacob Barker
Samm Metcalfe
Ashley Shumaker

ME 486C – Fall 2018
Instructor: Sarah Oman
Faculty Advisor: David Willy

Disclaimer

This report was prepared by students as part of a university course requirement. While considerable effort has been put into the project, it is not the work of licensed engineers and has not undergone the extensive verification that is common in the profession. The information, data, conclusions, and content of this report should not be relied on or utilized without thorough, independent testing and verification. University faculty members may have been associated with this project as advisors, sponsors, or course instructors, but as such they are not responsible for the accuracy of results or conclusions.

Table of Contents

1 Background

1.1 Introduction

A hands-on classroom experience can be vital for a college student's understanding of course material. This project's main goal is to help bridge the gap between figures and equations on paper to a functioning model that a student can interact with. The team aims to create a Brayton Cycle demonstration unit for a Thermodynamics II class. The model is based on a Turbojet engine to provide a real-world application of the Brayton Cycle. This will also benefit students by showing how a cycle is applied in a real-world situation. The sponsor and client for the project is David Willy, an instructor at Northern Arizona University. Once completed, this model will elevate his lectures and give students a better understanding of the Brayton Cycle.

1.2 Project Description

Thermodynamics II (ME392) classes need in-class demonstration equipment to help teach specific topics. This project will aide in the understanding of a specific cycle that will be determined by the client and team. For this project, one or more working benchtop examples are required to help with instruction. An example of a system within the design space that the client has in mind can be found here: https://www.youtube.com/watch?v=6rX4xv5-NvE&feature=youtu.be. Note that this is just an example and should NOT be directly copied. Client Requirements

- Must be able to operate in a safe manner for classroom demonstration
- Must not function from combustion (compressed air or electrical source is acceptable)
- Must be able to demonstrate at least one application (turbofan, etc)
- Must be mounted onto a cart for ease of transport in and out of the classroom
- Must be powered from typical wall outlet sources or be self powered
- Should be able to collect data to analyze performance
- The system does not have to work exactly as in the real world, but a user should be able to convert the testing results so it can be compared to a real world system
- Should be able easy to identify subsystems and functions of those subsystems within the demo unit

Client Based Deliverables

- At least one functioning system with data collection
- User's manual for operation
- Supporting Literature for system and subsystem functionality
- Short video demonstration in support of the User's Manual

2 Requirements

As noted previously, the customer for this project is David Willy, an Instructor at NAU, who intends to use this model as an in-class teaching tool. In designing this device, we wanted to ensure first and foremost that it meets his wants and needs for his intended usage. Thus, as a starting point, we first met with our client several times to determine what was most important to him. Using these client needs as well as the project description, we generated a list of customer requirements, and subsequently a list of engineering requirements to ensure these customer requirements were met.

2.1 Customer Requirements (CRs)

After meeting several times with Mr. Willy, reviewing the project description, and discussing the problem, the team came up with the following list of customer requirements (CRs), presented in Table 1 for reference.

Table 1: Customer Requirements

Scaled
Portable
Interactive
Educational
Usable in a lecture
Safe
Wall outlet or self-powered
Instructions for use
Durable/Reliable

The client's biggest priority was for the model to be interactive. To accomplish this, he had several specific requests. The model must take temperature and pressure measurements at the four key states in the thermodynamic cycle, and it must be transparent to allow students to see its inner-workings. Our team generated several more customer requirements based on this request: educational and usable in a lecture. For this model to be beneficial it must add a teaching element that a lecture alone cannot accomplish. Furthermore, the model must operate within the timeframe of a lecture, so its operation time cannot be exceedingly long. It must also be scaled, portable, and fit on a cart for transport into and out of a classroom. The model must also include instructions so that any instructor or student is easily able to operate it. The model must be reliable, so that it operates the same way every time, and durable, so that it lasts for many semesters of instruction. A model that only works intermittently or breaks after just a few uses would not be a worthwhile investment. Finally, the model needs to be safe for both the instructor and the students. To ensure safety and compatibility in the classroom, the model must receive power from a standard wall outlet or be self-powered.

2.2 Engineering Requirements (ERs)

With the list of customer requirements established the team sought to create measurable Engineering Requirements (ERs) to meet all customer needs. Table 2 provides a summary of these requirements.

Table 2: Engineering Requirements

Fit inside 2x3 perimeter
Total weight ≤100 lbs.
Measure pressure and temperature at every stage
Demonstration time ≤ 15 minutes
Clear outer casing
Use 120v AC, 60 Hz, and/or compressed air tank
Minimize exposure to dangerous or moving parts
Must last ≥ 10 semesters

To make the model scaled and portable, the team decided that the model should fit within a 2'x3' perimeter and should weigh less than 100 pounds. This was a rough estimate based on an average cart size that would be suitable in the classroom. The weight was a large overestimate but ensured the model would be movable by a single person when placed on a cart. The ER describing the ability to measure temperature and pressure at every state came directly from a customer request. This makes the model interactive and adds to its educational value. In analyzing Brayton Cycle problems, pressure and temperature are the first pieces of information needed, so these measurements are crucial to the effectiveness of this model.

To further enhance the educational aspect of the design, the team decided that the outer casing must be constructed from clear material to allow students to visualize how the model runs and how the cycle operates. To ensure the model is usable within a lecture, the team limited its total operation time to 15 minutes. The team also decided the model should be powered by 120v, 60Hz electrical power and/or compressed air, so that it can be easily and safely powered in the classroom. To further enhance safety, the team also agreed that there should be minimal exposure to any dangerous or moving parts; all moving components or those carrying electricity would be properly covered.

To address reliability and durability, the team created the ER that the model must last 10 semesters minimum. Ideally the model would last much longer, but the team felt that a five-year period would allow the model to fulfill its purpose and provide sufficient time for the investment costs to be recuperated.

2.3 Testing Procedures

The team also developed a set of procedures to test each requirement to ensure they are met. Some of the engineering requirements are quite easy to measure, such as size and weight. These can be measured with a simple tape measure and scale, although to measure weight the team will likely measure large components (turbine, cart, air compressor, etc.) separately, then sum the weights to calculate a total. Temperature and pressure measurement are also simple to test; the team will simply verify each sensor is collecting a reading that compares well with expectations (e.g. the ambient temperature and pressure should match local data). To test demonstration time, the team will run through an entire cycle of the device, from initial startup to data acquisition, to verify the cycle can be completed in the allotted 15 minutes.

To test safety, our team created a two-part test. First, the team will perform a visual inspection of the device to make sure everything is installed and fastened down correctly. If necessary, the team will adjust fasteners and joints. Next, we will enclose the testing area in a thin material, most likely tissue paper, and start up the device, allowing it to run through the cycle. If the device damages the lining, it will be evident that there is a safety issue somewhere in the design. However, if the paper remains undamaged, the device should be safe to use. The only issue with this test may be the exhaust at the turbine exit, so we may need to alter this test somehow in this location.

Testing reliability will be more difficult, as we will only be able to test the device when it is new. However, to predict reliability, we will simply perform numerous test cycles of the device to monitor its performance over time. The team set a goal for the device to last about 10 semesters. This device will most likely only be used about 4-5 times per semester, for a total of about 50 uses. To test this, the team will run through 25 test cycles with the device. We will watch to ensure all parts operate correctly, and check measurements to verify that they do not change over time, indicating a sensor error.

Finally, our team plans to test performance characteristics of the device, such as wind speed and/or thrust, and heat transfer of the heating element during operation. Ideally, this model should provide temperature and pressure differentials large enough to provide useful data, as well as a work output in the form of thrust. Measuring the efficiency of the combustion chamber will be done with an infrared thermometer, and wind speed and thrust will be measured using an anemometer and potentially a strain gauge.

2.4 Design Links

This system has gone through several design iterations to meet each of the previously mentioned engineering requirements. The total length of the system will be around 25 centimeters at most, leaving plenty of room on the cart for the pressure taps and thermocouple wiring. In addition, there are two shelves in the cart, so the upper shelf can hold the system while the bottom shelf can hold the compressed air tank, which also is small enough to fit on the cart. By far the heaviest component of the design is the compressed air tank, weighing around 20 pounds. The weight of the other parts in the system are negligible in comparison, so the design is well under 100 pounds. The system has two intrusive pressure and temperature measurement points before and after the combustion chamber. Then there are materials and set up in place to measure the ambient pressure and temperature, and the final pressure and temperature, for a total of 8 measurements—two at each state. The air compressor tank charges in about 6 minutes and discharges in less than 1, so if the system was demonstrated in class with charging it would take less than 15 minutes. The outer casing of the system will be a clear acrylic tube. The system runs on compressed air, which in turn gets power from a standard wall socket. Any moving parts of the design will be encased in the clear tube for minimal exposure. Finally, extensive use of pre-manufactured materials should ensure reliability and longevity, and easy repair.

2.5 House of Quality

After generating a list of engineering requirements, a Quality Functional Deployment (QFD) or “House of Quality” was used to determine which were most important. To begin, the team rated each customer need on its level of importance on a scale from one to five. Next, each engineering requirement was rated based on its effect in meeting the customer needs. A score of 1 indicates a weak relationship, 3 indicates a moderate relationship, 9 indicates a strong relationship, and a blank indicates no relationship. These relative scores were multiplied by the respective weights for each customer need and summed to calculate the Absolute Technical Importance. The Relative Technical Importance is simply an ordinal ranking of the

engineering requirements based on their absolute technical importance. Figure 1 displays the completed QFD.

Customer Requirement	Weight	Engineering Requirement	Size constraint	Weight	Measure inputs/outputs	Operation time	Outer casing	Power source	Minimize exposure to moving parts	Lifespan
1. Scaled	3		9	3				1		
2. Portable	4		9	9		1				
3. Interactive	2		1		9	1	9			
4. Eductational	5				9	3	9			1
5. Safe	5							1	9	
6. Usable in a Lecture	5		3	1	3	9	3	1		3
7. Wall outlet or self-powered	4							9		
8. Instructions for use	3									1
9. Durable/Reliable	3							1		9
Absolute Technical Importance (ATI)			80	50	78	62	78	52	45	50
Relative Technical Importance (RTI)			1	5	2	3	2	4	6	5
Target ER values			2' x 3'	<100 lb	>2	≤15 min	clear	AC/air	n/a	≥5 yr

Figure 1: Completed QFD

The QFD revealed that the most important engineering requirements were the size constraint, temperature and pressure measurements, and clear outer casing. This was expected, as all these engineering requirements ensure the educational aspects of the final design.

3 Existing Designs

Before beginning our own design, our team first began researching current systems that already exist. For this project, we decided to focus on two main areas of research. First, we researched the general processes behind the Brayton Cycle, as well as real word applications of this cycle. Next, we researched small-scale, simplified model units that would be more similar to what we intended to build.

3.1 Design Research

The team began research by investigating real-world applications of the Brayton Cycle. While there are countless variations of Brayton Cycle engines, they can be categorized into four main types: turbojets, turboprops, turbofans, and turboshafts. All four of these engines share the same core element: a gas generator consisting of a compressor, combustion chamber, and turbine section [1]. The turbojet is the simplest of the four types and is essentially just the gas generator described above with an inlet and exhaust nozzle added. The compressor, driven by the turbine, compresses air into the combustion chamber, where combustion adds a heat to the flow. The heat and pressure are converted into rotation to power the

compressor, and the remaining energy is then used to create thrust in the exhaust section. A turboprop operates on the same principle, except the excess energy remaining after powering the compressor is used to power another turbine section, attached to a propeller through a gearbox [1]. In a turboprop, the propeller generates most of the thrust rather than the exhaust nozzle in a turbojet engine. A turboshaft engine is nearly identical to a turboprop engine, except that the output shaft is not connected to a propeller. Instead, it can be used to power the rotor blades of a helicopter or connected to a generator such as in a power plant [1].

The turbofan engine is the most widely used type of engine for aircraft propulsion [1]. In a turbofan, excess shaft power is used to drive a fan ahead of the main compressor. The air from this fan passes around the inner core of the engine through a separate nozzle, which provides most of the thrust [1].

Our client initially requested that our group avoid building a turbofan model, so we debated between the other three types. Initially we intended to design a turboprop style model. However, given the small size of our design team, we ultimately decided it would be best to focus on the simplest type: the turbojet, which would provide a model of the Brayton Cycle without the added complexities of an additional gearbox and propeller.

3.2 System Level

3.2.1 Real-World Applications

Most modern-day aircraft have abandoned the turbojet engine in favor of the turbofan engine design. However, one application where turbojets are still frequently used is small unmanned aerial vehicles, like drones and cruise missiles. The compact size and relative simplicity of a turbojet engine makes it useful in these applications. Today, one of the leading manufacturers of turbojet engines is Safran, who produces the Microjet engine line. There are several different variations in this engine range, so the team decided to focus one type, the Microturbo TRI 60, to get an idea of turbojet engine specifications. The Microturbo TRI 60 is shown in Figure 2 [2].

Figure 2: Microturbo TRI 60 Turbojet Engine [2]

There are also several variations within the TRI-60 product line, but all variants share similar specifications. This turbojet engine is approximately 26 inches long, 13 inches in diameter, and weighs between 108 and 135 pounds. It makes use of a three-stage, axial turbine, with a compressor pressure ratio ranging from 3.83:1 to 5.58:1. The combustor is an annular smokeless type, with 12 nozzles and a single spark igniter housed in a stainless-steel casing. The turbine is a single stage, axial design, and mates directly to the compressor through a single shaft. The turbine inlet temperature is approximately 1,850 °F [2]. These design specifications yield thrust ratings of between 787 and 1,200 lbst depending on the model variation.

The Microturbo TRI 60 engine has been used in many applications, from Anti-ship missiles to Drones [2]. This research was very surprising to the team. The TRI 60 turbojet is small enough to meet the target size specified in our engineering requirements and can still generate over 1000 pounds of static thrust. While this engine is far more complex than anything our team could produce, it was valuable in determining some design criteria for our design. It also reveals how compactly turbojet engines can be manufactured.

3.2.2 Existing Demonstration Units

One of the most interesting products discovered during our research was the MiniLab Gas Turbine Lab made by Turbine Technologies [3]. This is a self-contained turbojet engine demonstration unit, which essentially has the same intended use as our project. As shown in Figure 3, the MiniLab Gas Turbine Lab consists of a small-scale SR30 Turbojet engine, mounted inside of an enclosed workbench. The apparatus is mounted on wheels to allow for easy transportation and is shielded to protect users from heat and moving parts.

Figure 3: MiniLab Gas Turbine Lab [3]

This product measures temperature and pressure at every state, which is an essential customer need for our design. It also includes its own software program, which can be used to display these pressure and temperature readings, as well as fuel flow, thrust, and engine speed, shown below in Figure 4. Additionally, the software allows users to plot any of the measurable parameters to learn how the performance reacts to the operating conditions.

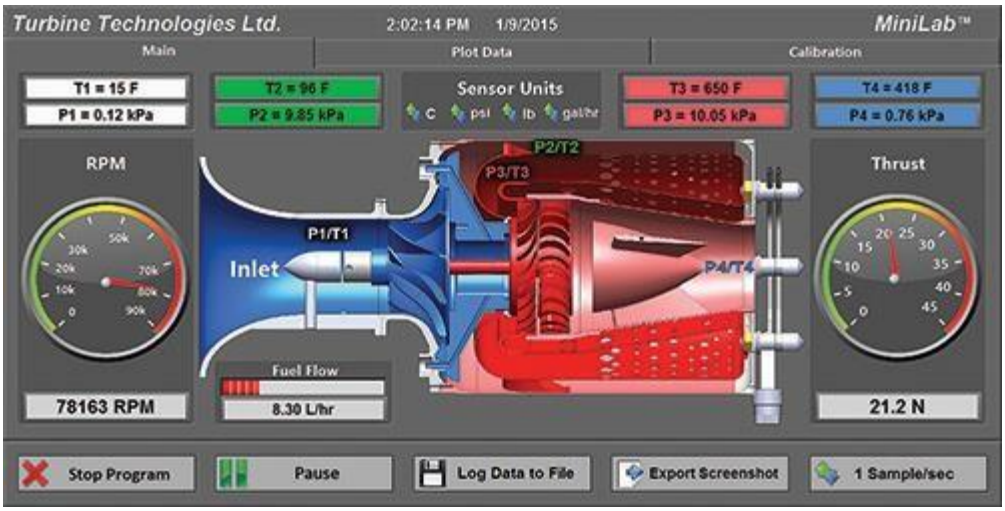

Figure 4: MiniLab Interactive Virtual Instrument Panel [3]

This product is essentially the ideal version of a Brayton Cycle demonstration unit and meets or exceeds all customer needs given to our design team save for its large size. Unfortunately, this device was far more complex than any design our team could produce and also far too expensive. However, it provided a valuable benchmark which demonstrates how a model like this should operate. Additionally, the team also felt that there were several ways this design could be improved upon. For example, given that the MiniLab uses a real turbine engine, the user cannot see any of the moving parts inside of the turbojet engine. While our design is not as realistic as this product, it does have one advantage in that the clear outer casing allows students to visualize what is actually happening during the operation of the Brayton Cycle. Additionally, it is much smaller and more portable, and significantly more affordable.

3.2.3 Other Applications

During research our team also found that there are fully-functional scale models of turbine engines used for model airplanes. These small replicas function as real engines and use actual fuel and combustion. At the time of this research, the team was still planning on building a turboprop engine, and focused on this type of engine. One example of a model turboprop is the Wren Power Systems Model 54 turboprop engine, which is shown in Figure 5.

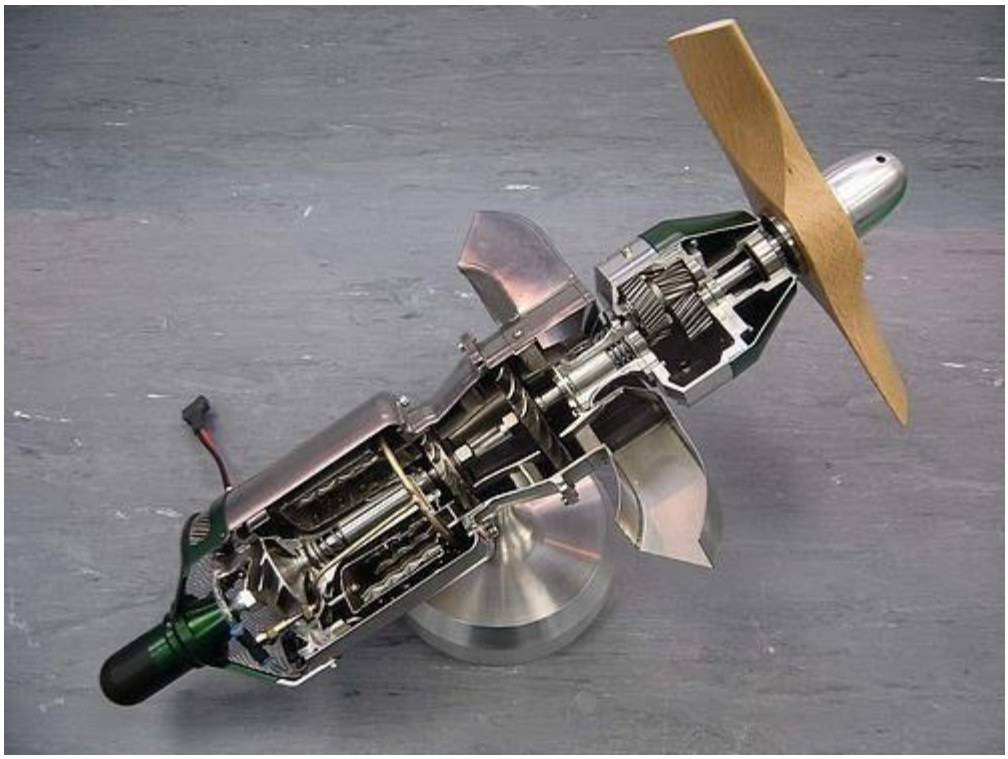

Figure 5: Wren 54 turboprop cutaway [4]

The engine utilizes a single compressor and two turbine stages. The first turbine is used only to power the compressor. There is a second, separate shaft with a single turbine that drives the gearbox for the propeller. This design is called a two-stage engine because of the separated turbine stages, which can be seen in Figure 5 above. In this model, the intake is on the opposite end of the propeller, which is a less common design. Real turboprop engines usually have the intake behind the propeller to help force more air in the compressor. Because of this engine's size it is extremely sensitive to foreign particles and the reversed design is preferable, as the intake will be inside the cab of the plane and will allow cleaner air to enter the compressor. This two-stage design is less efficient than a single-stage design where the output shaft of the turbine is directly connected to the gearbox. This is because the second turbine is an impulse turbine relying on the air being exhausted to spin the shaft causing greater losses than if the shaft was directly connected to the gearbox [5]. Another peculiarity of this design is the use of a radial compressor rather than a typical axial compressor. In this application, the radial compressor is advantageous, as it can be implemented using a single stage. This parameter is discussed in more detail in the Compressor section.

These model turbines are visually impressive and the cutaway shown above would make an excellent teaching tool. Unfortunately, however, they are very expensive; Wren Power Systems website lists the model shown above costs around $4,000, which was far outside of our team's budget [5]. Still, it was beneficial to find this model, as it showed an example of a Brayton Cycle model very different from the typical design. This showed our team that we could alter the standard design to better suit our application.

3.3 Subsystem Level

As mentioned previously, all Brayton Cycle engines, including turbojets, turbofans, turboprops, and turboshafts, share a similar core element known as the gas generator, which consists of a compressor, combustion chamber, and turbine section. Thus, in performing subsystem design research, the team decided to focus on these three elements.

3.3.1 The Compressor

The compressor is the first component in a Brayton Cycle engine. It connects through a shaft to the turbine, from which it receives its power. The purpose of the compressor is to compress the air and raise its pressure before combustion to stretch the pressure vs. volume (P-V) diagram as well as the Temperature vs. Entropy (T-S) diagram, increasing work output.

There are several ways to compress air in a Brayton Cycle engine. The standard type seen in most jet engines today is the axial compressor. This configuration is composed of radial vanes (or blades) that are mounted like discs on a central hub, which directs the flow through the compressor parallel to the shaft [6,7]. Figure 8 shows a simple diagram of an axial flow compressor with stator vanes, which will be discussed later.

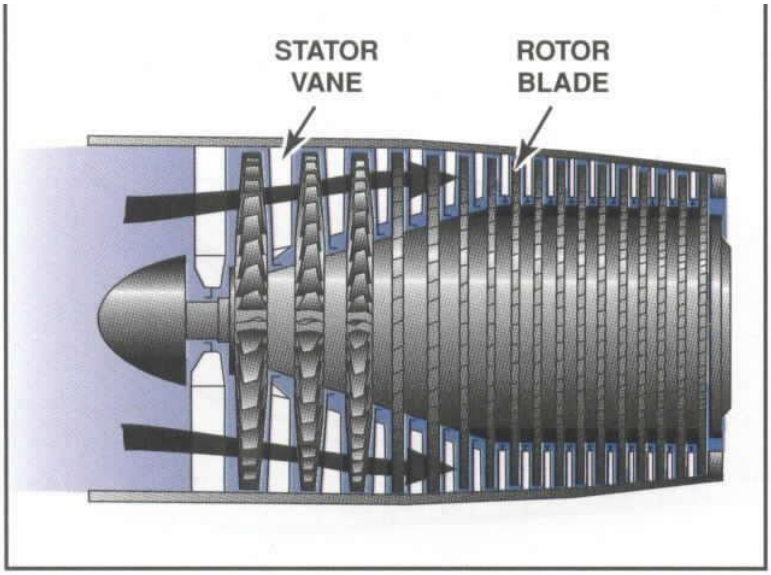

Figure 8: Cross section of an Axial Compressor [7]

As shown above, the rotor blades look similar to fan blades, and rotate to draw air into the engine. As the flow moves further into the engine, the area between the rotor hub and outer casing decreases, which compresses the air. This compressed air flow is then directed to the combustion chamber.

The stators do not rotate with the rest of the blades, and while a functioning compressor can be made without them, stators increase the efficiency and effectiveness of each stage. A single compressor stage is defined to have one set of rotors and one set of stators [8]. The rotating blades will cause the flow to swirl in the direction of rotation, which causes the compressor to be less efficient. A simple diagram of one rotor in a cylindrical housing and how the flow swirls can be seen in Figure 9 below.

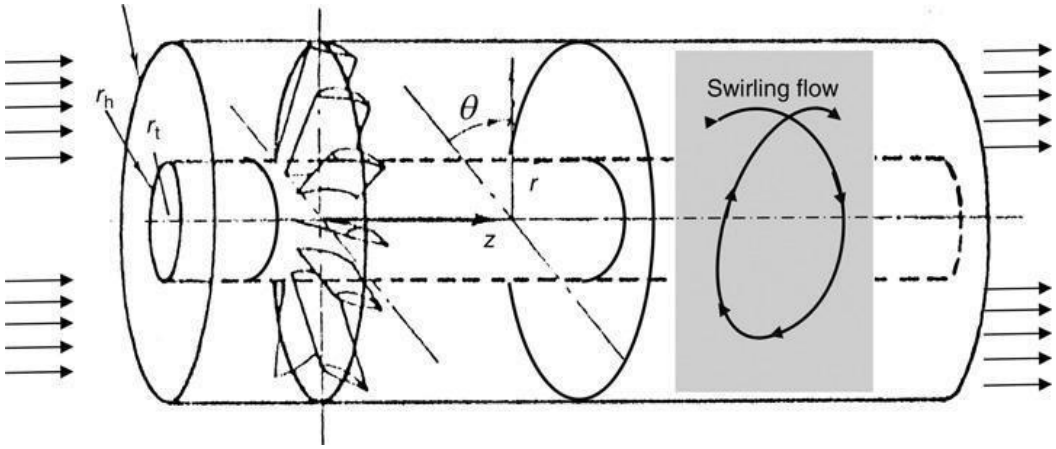

Figure 9: Flow swirl due to rotor [9]

Adding stator blades redirects the flow to be parallel to the axis of rotation. This decreases turbulence in the flow, increases the static pressure of each stage, and directs the flow perpendicular to the blades of the next stage.

The decrease of area between the inner hub and outer casing is an essential part to effectively compressing flow in an axial compressor. To achieve this area-decrease, the diameter of the hub can change, the outer diameter of the casing can change, or both can vary; the design in Figure 8 uses a combination of both to accomplish the area decrease. The first section, closest to the inlet on the left, has a constant outer casing diameter while the hub has a converging cross section. Next, the center section has a combination of a changing outer casing and inner hub radii. Lastly, the far right section has a constant hub radius with a converging outer casing. A more in-depth look at the relationship between the hub and outer casing can be seen in the turbine section.

Another compressor configuration is the radial, or centrifugal, compressor. Unlike the axial compressor, this configuration relies on the swirling of air to function, which forces the air away from the rotor and down to the combustion chamber. This configuration is mainly used in turbochargers in the automotive industry, though it can be used in a Brayton Cycle engine as seen in the model turboprop shown in Figure 5. It was also implemented in early jet engines [6]. Figure 10 below shows the rotor and housing of a radial compressor.

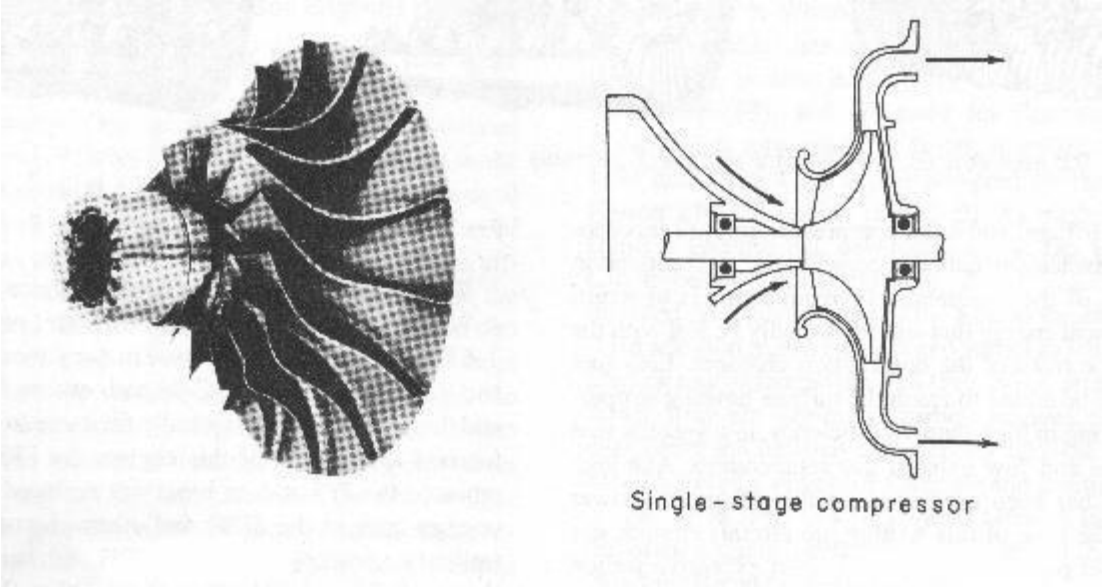

Figure 10: Cross section of Radial Compressor

As Figure 10 demonstrates, the vanes of a radial rotor direct the air from the center of the rotor to the outer edges. This configuration is ideal when using only one compressor stage as one radial stage is much more effective at compression than a single axial stage [6]. One NASA article states that an average axial compressor stage can increase the pressure by about 1.2 times, where a similar single-stage radial compressor stage can compress the air by a factor of 4 [6]. Though they are simpler and more efficient, radial compressors cannot be placed in series the same way as axial compressor stages. To place radial compressor stages in series, the flow must be redirected to the center of the next stage for the rotor to be effective.

Based on this research, our team decided an axial compressor would likely be the best option for our design. This is detailed in the design selection stage, which is later in the report. Because our design is to be used as an educational tool, and is supposed to represent how an actual Brayton Cycle engine works, we decided against the radial compressor, as they are rarely used in actual jet engine applications.

3.3.2 The Combustion Chamber

The main purpose of the combustion chamber is to add heat to the system before the working fluid enters the turbine. This increased temperature gradient increases the potential work output from the turbine. In a typical design, air is mixed with a fuel source and ignited in the chamber. There are typically three different geometric shapes for combustion chambers [10]. The Can Combustor, Figure 11, is made of several different chambers through which air flows [10]. Each chamber has outer and inner tubes; the inner tube is where the combustion takes place and the air flows through the tube by louvers in the inner dome [10]. The outer tube is used to regulate air flow [10].

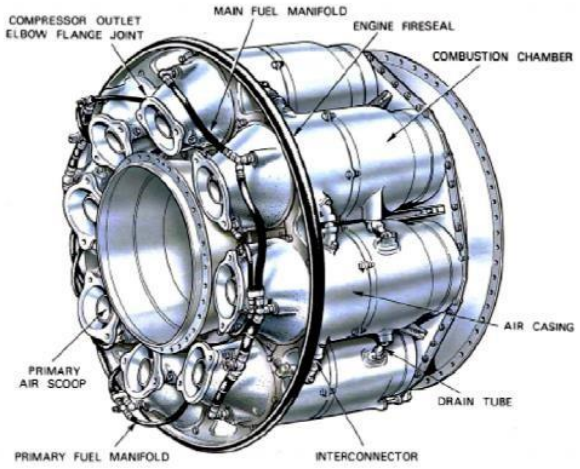

Figure 11: Can Combustor

An annular combustor, Figure 12, has a single chamber with walls inside to control the air flow into the combustion zone [10]. There are two areas where the compressed air is mixed with the fuel. The primary air supply is fed into the combustion chamber to mix with the fuel source and combusted [10]. The secondary air is used to cool the air-fuel mixture before entering the turbine to prevent damage to the turbine blades [11].

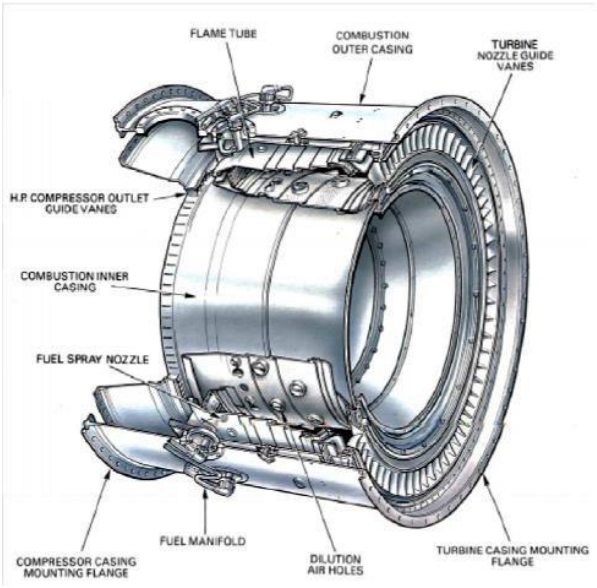

Figure 12: Annular Combustor

The third type of combustion chamber is the Can-Annular combustor, which combines the two previous types as the name suggests [10]. This combustor takes the several chambers of a can combustor and incorporates an annular combustor in each chamber [10]. This is shown below in Figure 13.

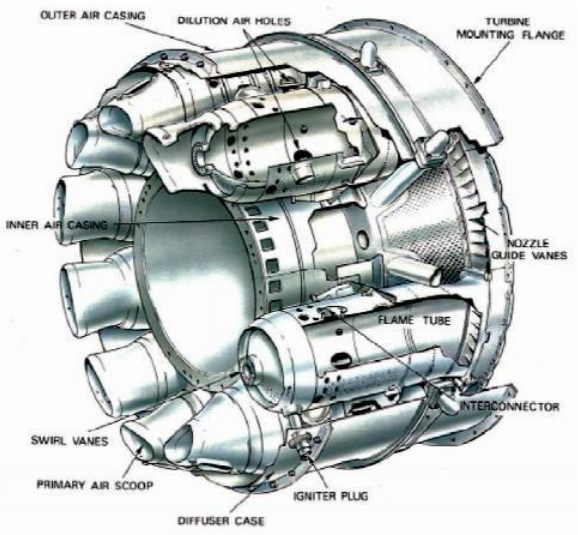

Figure 13: Can-Annular Combustor

For any combustion chamber to work properly, the air velocity coming into the chamber must be decelerated with a diffuser to ensure a stable combustion [10]. Too much air in the combustion chamber will cause a lean mixture, preventing the engine from operating at maximum efficiency. The air-fuel ratio that will yield the best efficiency is approximately 1:15 [11].

For safety reasons the team cannot create a model with a functional combustion chamber. The team decided to research outside sources to simulate the effect of an actual combustion chamber. There are several methods of accomplishing the effects of a combustion chamber. One way is to add more compressor stages to increase pressure. Another option would be to have an outside heating source pump in heated air or to have heated coils in place of the combustion chamber. The engine would still benefit from the use of a diffuser before the simulated combustion chamber to create the most heat transfer into the system.

In both a real or simulated combustion chamber, the design must be such to keep the total pressure loss at a minimum. In any design there will be losses due to friction [11]. Designing for minimal pressure loss could include making the surfaces of the combustion chamber as smooth as possible and making the air flow as streamlined as possible. For an actual combustion chamber, pressure losses are usually around 2-7 percent [11].

3.3.3 The Turbine

The turbine sits behind the combustion chamber and is mounted on the same shaft as the compressor. Its primary task is to power the compressor, by converting the heat and pressure energy from the combustion chamber into mechanical shaft power [12]. The use of the remaining power depends on the type of application, which heavily influences the final design. However, there are several design options used no matter the application.

The Turbine stage of a gas generator contains two primary types of components: the turbine nozzle, or stator, and the turbine rotor. The turbine nozzle is a row of stationary blades mounted ahead of the rotating rotor. Because it is stationary, the stator cannot do any work. Instead, it has two main functions. First, it converts the potential energy in the hot, high-pressure gas into kinetic energy by adding swirl to the flow [12,13]. Second, the turbine nozzle changes the direction of the flow, in order to maximize the force it can impart onto the turbine rotor. Generally, a turbine nozzle is placed ahead of each rotor to redirect the flow before each stage. An illustration of this configuration is shown in Figure 14 below.

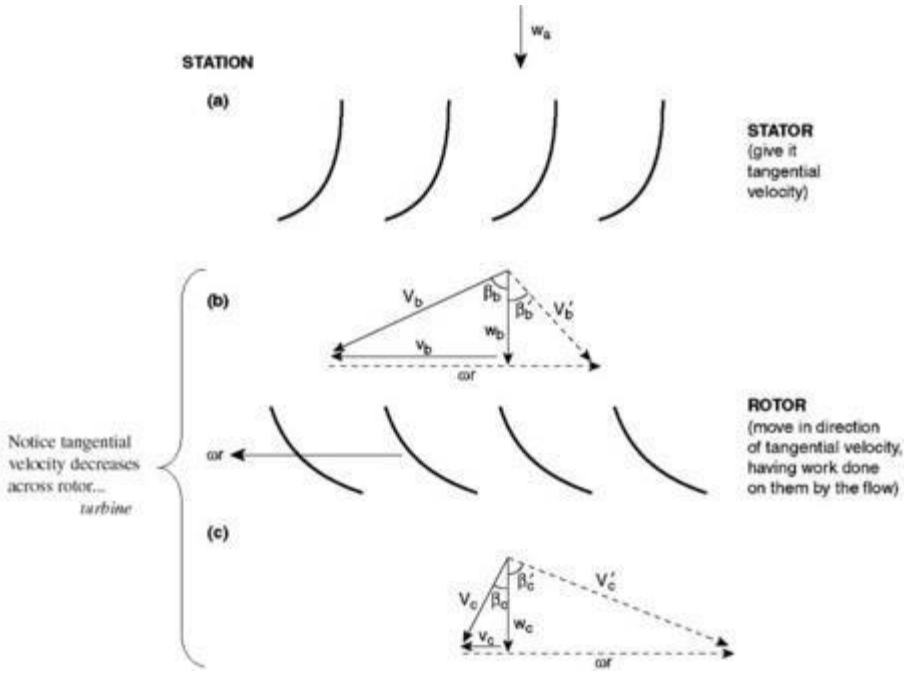

Figure 14: Turbine Stator/Rotor arrangement [13]

However, particularly for our design application, the turbine stator presented a manufacturing challenge. The stator stage must be mounted concentrically between the rotor stages but must be held stationary. In a real gas turbine, the stator can be incorporated into the outer casing of the engine, as shown in Figure 15 [14].


Figure 15: Turbine Stator [14]

However, because our design is intended for use as a demonstration tool, the engineering requirements dictate that the outer casing must be transparent. Most 3D printers can only produce opaque objects even with clear filament. Thus, we decided to use pre-manufactured acrylic tubing, which makes it difficult to install fixed stator sections. Initially, we to avoid this issue by using a stator-less turbine design. As the name suggests, a stator-less turbine removes the nozzle guide vanes, and the flow exiting one turbine rotor passes directly to the next rotor without the use of a stator in between [15]. While this design simplifies manufacturing, it adds complexity to the rotor blade design. Ultimately, we decided to incorporate stators using a press-fit design, which is detailed later in the report.

There are two major classifications for turbines: Impulse, or constant pressure turbines, and Reaction Turbines [12]. In an Impulse Turbine, gas expansion occurs only in the stator, or turbine nozzle, which converts potential energy in the gas from heat and pressure into kinetic energy. As the gas passes through the nozzle guide vanes, it is accelerated rapidly while its temperature and pressure decreases. The gas then exits the turbine nozzle, impacting the turbine blades, and imparting rotation through momentum exchange [12]. As the gas passes through the rotating stage of the turbine, its pressure remains constant, hence the "constant pressure" name. After each turbine stage, velocity is lower than at the nozzle exit, as energy has been extracted from the flow and converted into shaft work. This process can be observed in the plot on the upper left of Figure 16, which illustrates how pressure, temperature, and velocity change as the flow progresses through the different stages of the turbine [12].

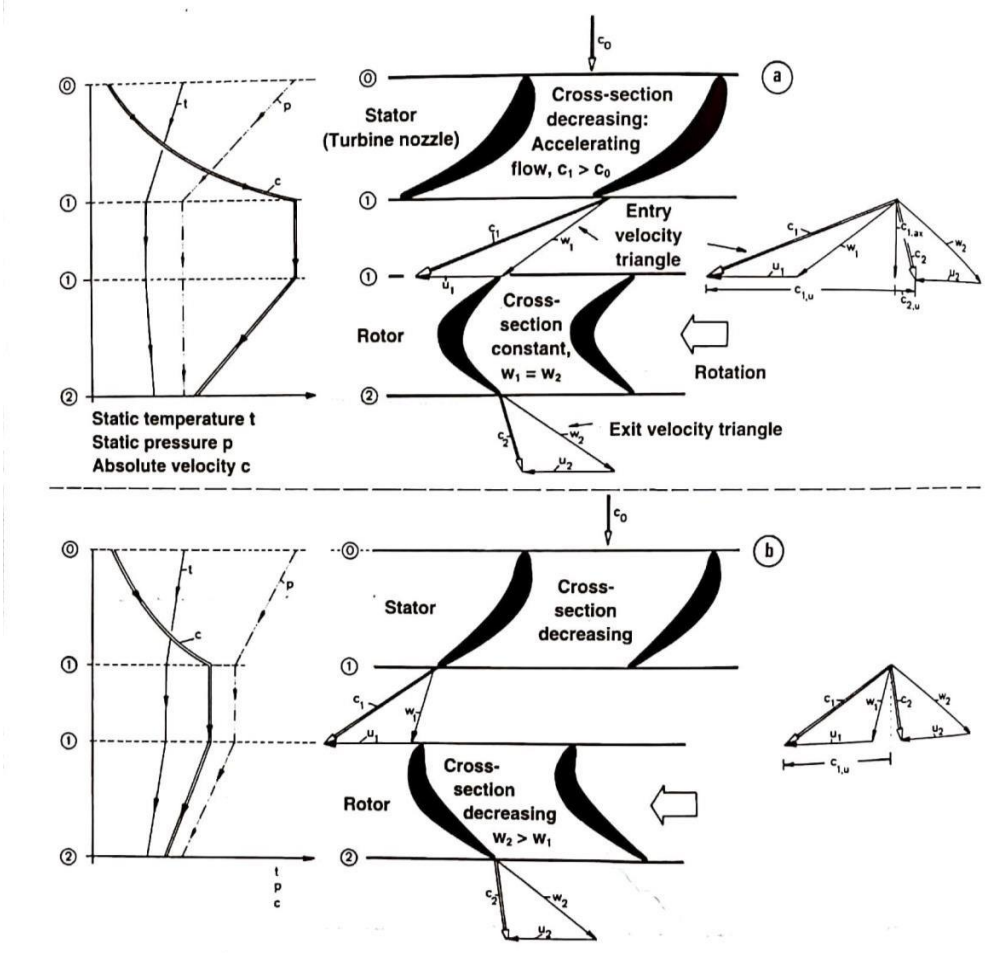

Figure 16: Impulse vs. Reaction Turbine [12].

Alternatively, in a Reaction Turbine, gas expansion takes place in both the stationary nozzle and the rotating turbine [12]. In the rotor section, the gas expands and accelerates similar to the Impulse Turbine, but to a lesser degree. This expansion continues in the turbine section, where the rotating blades share a more similar profile to the guide vanes. Due to the nature of the blade profile design, the air flow creates an aerodynamic force on the turbine blades, much like the lift force on a wing, which causes the turbine to rotate [12]. However, there is still a momentum exchange between the gas and the blades, much like in the Impulse Turbine.

A comparison of these two designs and their respective blade profiles is provided in Figure 16. The plots on the left of the figure compare the differences in pressure, temperature, and velocity through the different sections. Both of these designs have their own benefits. The Reaction Turbine is generally more efficient, but an impulse turbine has a higher power output, which can reduce the number of turbine stages required [12].

Given the benefits of each design, most turbines use a combination of the two. In a turbine, circumferential velocity increases radially outward, from a minimum at the hub to a maximum at the blade tip. However, it is beneficial to have a constant velocity profile across the entire length of the blade. To accomplish this, turbine blades are generally designed as constant-pressure type at the base, gradually changing to the reaction-type at the tip [12].

Another consideration of turbine design is the profile of the hub and casing. These choices can affect mass flow rate, power production, and turbine efficiency [16]. Again, there is endless variability in designing these parameters. However, the options can be divided into three main categories: constant tip radius with variable hub radius, constant hub radius with variable tip radius, and variable hub and tip radius [16]. These three designs are presented in Figure 17 for comparison.

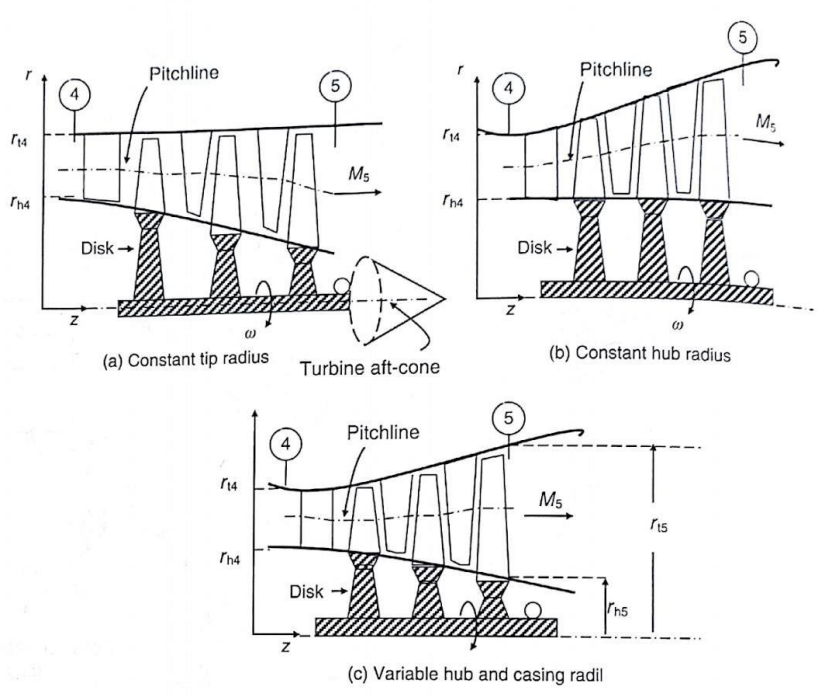

Figure 17: Turbine Hub and Casing Options [16]

Each of these designs offer their own distinct advantages. For instance, a constant tip radius can be beneficial in a turbofan. In a turbofan engine, the hot exhaust is mixed with the "cold" stream from the outer

flow. In this scenario, using a constant outer radius can lead to better integration of the cold and hot air streams [16]. A constant outer radius also reduces centrifugal stresses in the rotor blades, and can reduce the weight and frontal area of the engine. In aircraft engines, a tapered hub radius can also be advantageous, as the hub can be integrated with the exhaust cone, which is used to direct exhaust flow at the turbine exit [16].

A constant hub radius also has several benefits, particularly in stationary gas turbines used in power plants. This design choice can integrate with an exhaust diffuser, and also reduces manufacturing cost and complexity since all turbine rotor disks share the same inner diameter. Using both a variable hub and tip radius can allow for a constant pitchline. However, it is also the most complex design, the most difficult to manufacture, and generally increases both cost and weight [16].

As mentioned earlier, our design uses pre-manufactured acrylic tubing for turbine housing. Because of this, it was not possible to use a variable casing radius design. Thus, our design uses a variable hub radius to accomplish area reduction in the compressor and expansion in the turbine. The hub radius is easily changed using 3D printing, allowing the outer casing to remain constant and completely transparent for easy viewing.

4 Designs Considered

In the initial decision process, we decided to focus on the main structure of the design. Though there are just three main subsystems to any Brayton Cycle engine, there are many ways to build each subsystem. Each team member researched one subsystem and generated a few variations that could be used in our design. The team then worked to create different combinations of these subsystem designs to create a total of 15 different concepts. Most of these designs combined different design elements discussed in the above subsystem research. The design team considered compressor and turbine type, hub and casing geometry, shaft configurations, and different options for combustion chamber substitutes. We sketched each of the 15 concepts, which can be seen in Appendix A.

Table 3: Design Descriptions

Design description
1. Radial compressor and turbine, no heating
2. constant hub radius, no heating, statorless
3. constant hub radius with preheat, statorless
4. Constant tip radius with preheat, statorless
5. Constant tip radius with heating in chamber, statorless
6. constant tip radius with heating around outside of chamber, statorless
7 .Concentric shaft, 2 separate stages of comp. and turb. with preheat, statorless
8. Front Diffuser, constant tip radius with preheat, statorless
9. Stator compressor and turbine, constant tip radius with preheat
10. Stator compressor turbine, constant tip radius with in chamber heat
11.Statorless, constant hub radius, with heating around outside of chamber
12. Statorless, constant hub radius, with in chamber heating
13. Constant inner and outer radius, statorless, no heating
14. Stator compressor and turbine, constant hub radius, with preheat
15. Stator compressor and turbine, constant hub radius, with pre-chamber heating

Design 13 is highlighted in yellow as it was chosen as the datum when used in design selection, discussed further in Section 5.1. The chosen datum was the simplest design possible, which used constant a constant hub and tip radius, stator-less blades, and no added heating in the combustion section. The design sketch for the datum can be seen in Figure 18 below.

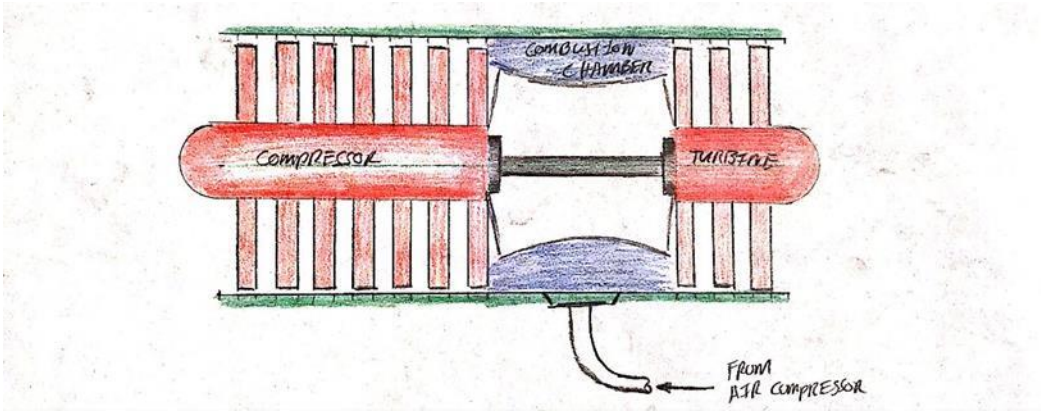

Figure 18: Detailed Sketch of Datum

Each concept utilized a different combination of the subsystem variations. For example, Figure 19 shows a sketch of Design 14, which used stators on the compressor and turbine. Figure 20 shows a sketch of Design 3 without stators.

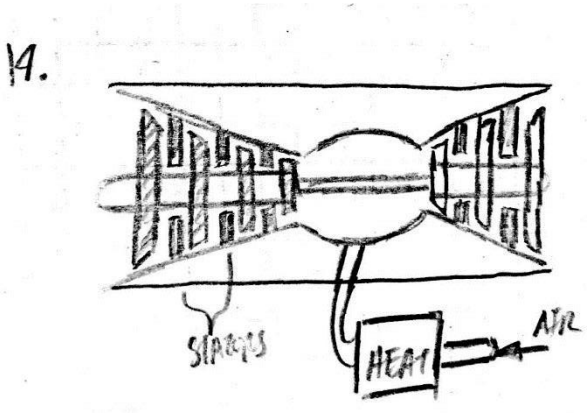

Figure 19: Design 14 Sketch

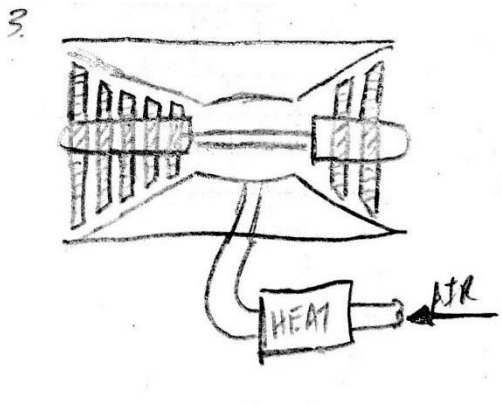

Figure 20 Design 3 Sketch

In Figures 19 and 20 above, both designs made use of a "pre-chamber" to heat the incoming air, and both designs utilize the constant hub radius design. To illustrate the different heating designs, Figure 21 below depicts Design 5 with the in-chamber heating, and Figure 22 below shows Design 11 with the heating around the outside of the chamber.

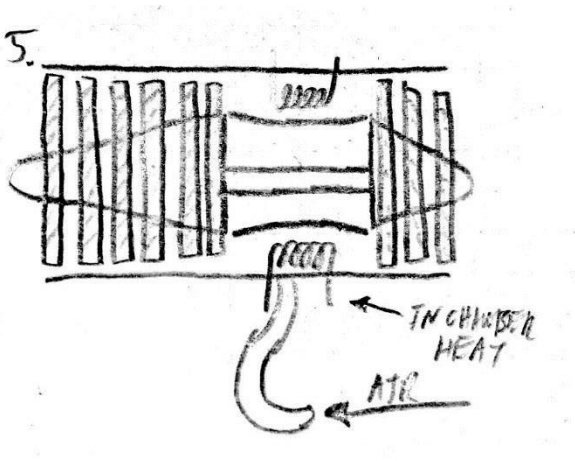

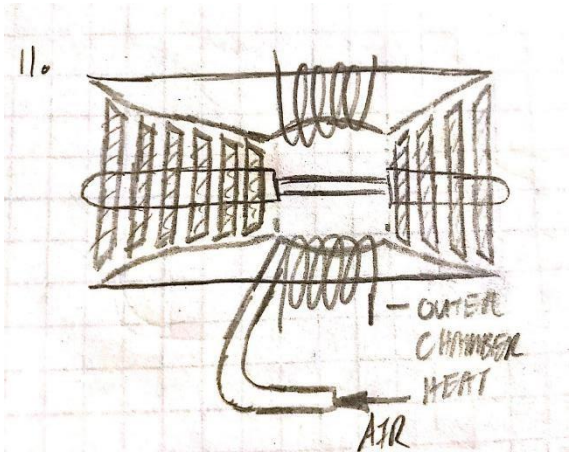

Figure 21: Design 5 Sketch

Figure 22: Design 11 Sketch

In the above figures it can also be seen that Design 5 utilizes the constant tip radius and Design 11 utilizes the constant hub radius.

5 Design Selected

Having created many potential concepts, our team needed a way to objectively choose the best design. This section details the decision-making processes implemented by the team to choose a final design from the initial fifteen concepts, as well as a brief discussion of the results of these methods. It then describes the finalized design in detail including engineering calculations used in the analysis.

5.1 Rationale for Design Selection

To reduce the number of potential designs, the team first compiled the 15 designs into a Pugh Chart and scored each against the engineering requirements and the datum to find the top four designs. The entire Pugh Chart can be seen in Appendix B. Below in Table 4 is small portion of our Pugh chart showing our requirements and how the first 4 designs scored.

Table 4: Pugh Chart showing designs 1-4

	1	2	3	4
Portable	-	s	s	s
Interactive	-	-	-	+
Educational	-	-	+	+
Durable	+	-	-	s
Reliable	-	s	-	-
Fit in 2x3 foot rectangle on cart	s	s	s	s
Total weight under 100lbs	-	s	s	s
Demo shouldn't take more than 15 minutes	s	s	-	-
Visability	-	-	-	s
Use 120v AC, 60Hz, and/or compressed air tank	-	s	s	s
Minimize exposure to dangerous/moving parts	-	s	s	s
Feasibility	-	-	-	-
Efficiency	-	+	+	+
Cost	-	-	-	-
Total -	11	6	7	4
Total +	1	1	2	3
Total s	2	7	5	7
	14	14	14	14

The red highlighting above the first three concepts indicates that they were eliminated in the first round of concept selection. The green highlight on the fourth design shows that it scored well enough to proceed to the next step in the process.

To decide on a final design, our team placed the four remaining designs into a Decision Matrix. The Decision Matrix used the same criteria as the Pugh Chart. However, several criteria were rated at "S" or same for all designs, so these were eliminated from the Decision Matrix to streamline the process. After narrowing the criteria, our team assigned a weight to each, based on its importance in meeting the customer needs. The criteria were weighted on a scale from zero to one, with the sum of all criteria weights summing to one. Next, each design was rated on a zero to 100 scale based on its competence for each of the evaluation criteria. Because the designs were highly conceptual at this point, most of these ratings were subjective. We found it most effective to compare the designs against one another when assigning scores. For instance, adding a heating element to the design will increase its educational value and efficiency, but will reduce its reliability and longevity.

After scoring all four designs, these raw scores were multiplied by the weight of each category, and summed to determine the strongest design. The completed Decision Matrix is shown in Table 5.

Table 5: Decision Matrix

	Concept	9		11		13		15	
Criteria	weight	raw score	wtd score	raw score	wtd score	raw score	wtd score	raw score	wtd score
Educational	0.2	65	13	80	16	50	10	80	16
Visability	0.18	80	14.4	65	11.7	80	14.4	80	14.4
Minimize exposure	0.13	50	6.5	50	6.5	50	6.5	50	6.5
Cost	0.13	80	10.4	75	9.75	85	11.05	75	9.75
Feasibility	0.1	50	5	70	7	90	9	70	7
Interactivity	0.17	60	10.2	60	10.2	70	11.9	80	13.6
Reliability	0.03	60	1.8	60	1.8	80	2.4	60	1.8
Durability	0.03	60	1.8	60	1.8	80	2.4	60	1.8
Demo time	0.02	80	1.6	80	1.6	90	1.8	80	1.6
Efficiency	0.01	85	0.85	70	0.7	50	0.5	70	0.7
Total	1		65.55		67.05		69.95		73.15

As shown above, all four final designs scored very closely, as all had many similarities. However, based on these criteria, Design 15 was the strongest concept. This is illustrated below in Figure 23.

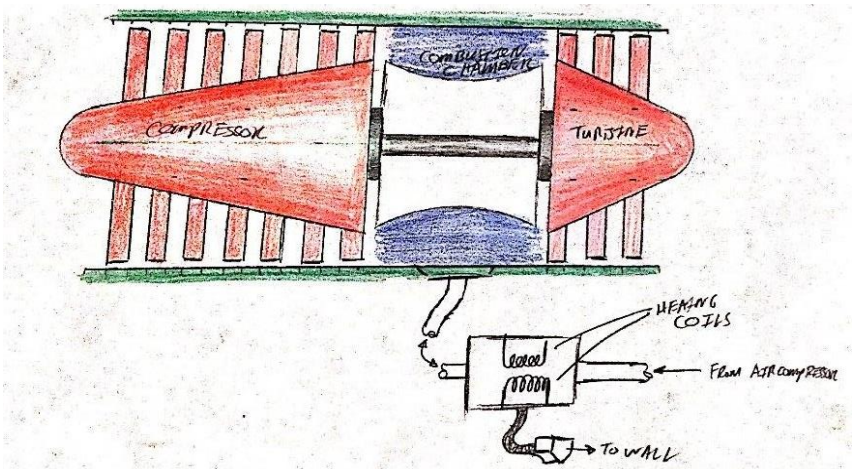

Figure 23: Winning Concept

This design functioned without any combustion, as did most others. It featured a stator-less compressor and turbine, with a constant blade tip radius and variable hub radius. Compressed air was used in place of combustion to add energy to the flow in the form of pressure. This design also implemented an in-line heater for the compressed air stream to further enhance the energy added during this stage.

The team saw numerous benefits in this chosen design. First, the elimination of combustion made this unit much safer to use in a classroom setting. Use of compressed air would sufficiently increase flow energy and adding a heater helped to differentiate further between measurements at different states. Heating the air before it enters the "combustion chamber" is also beneficial, as it prevents the plastic from being heated directly, theoretically reducing thermal strain and increasing longevity. Finally, a stator-less compressor and turbine were chosen with constant tip radius for simplifying manufacturing.

Ultimately, as the project progressed, many aspects of this design were changed based on later variables. However, this served as the starting point for the design, and many aspects in the final design are similar to this initial concept. Next, first iteration of the final design is presented, as well as additional analyses completed by the team.

5.2 Design Description

Figure 24 shows an isometric view of the final CAD model, while Figure 25 shows an assembly drawing. For detailed drawings of all components, please refer to Appendix C.

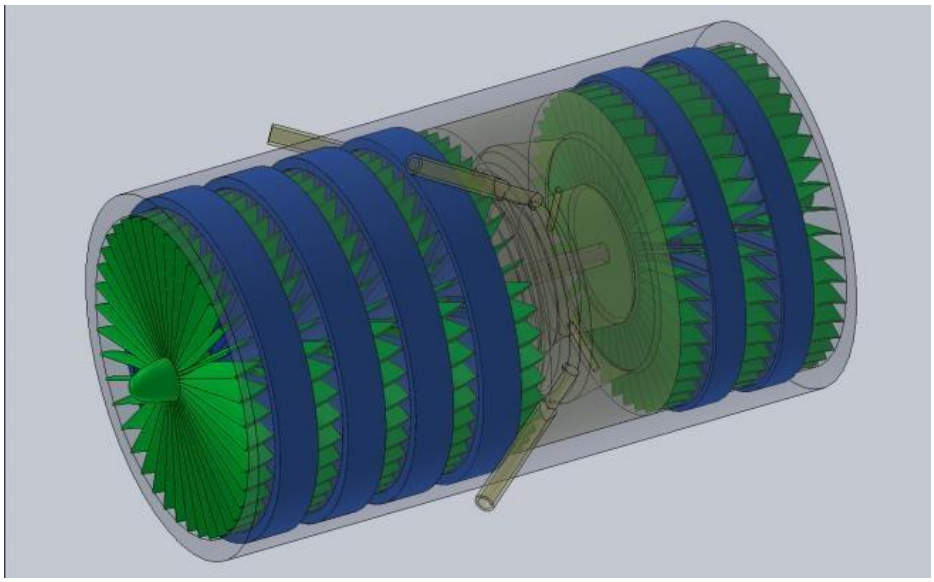

Figure 24: Final CAD Model

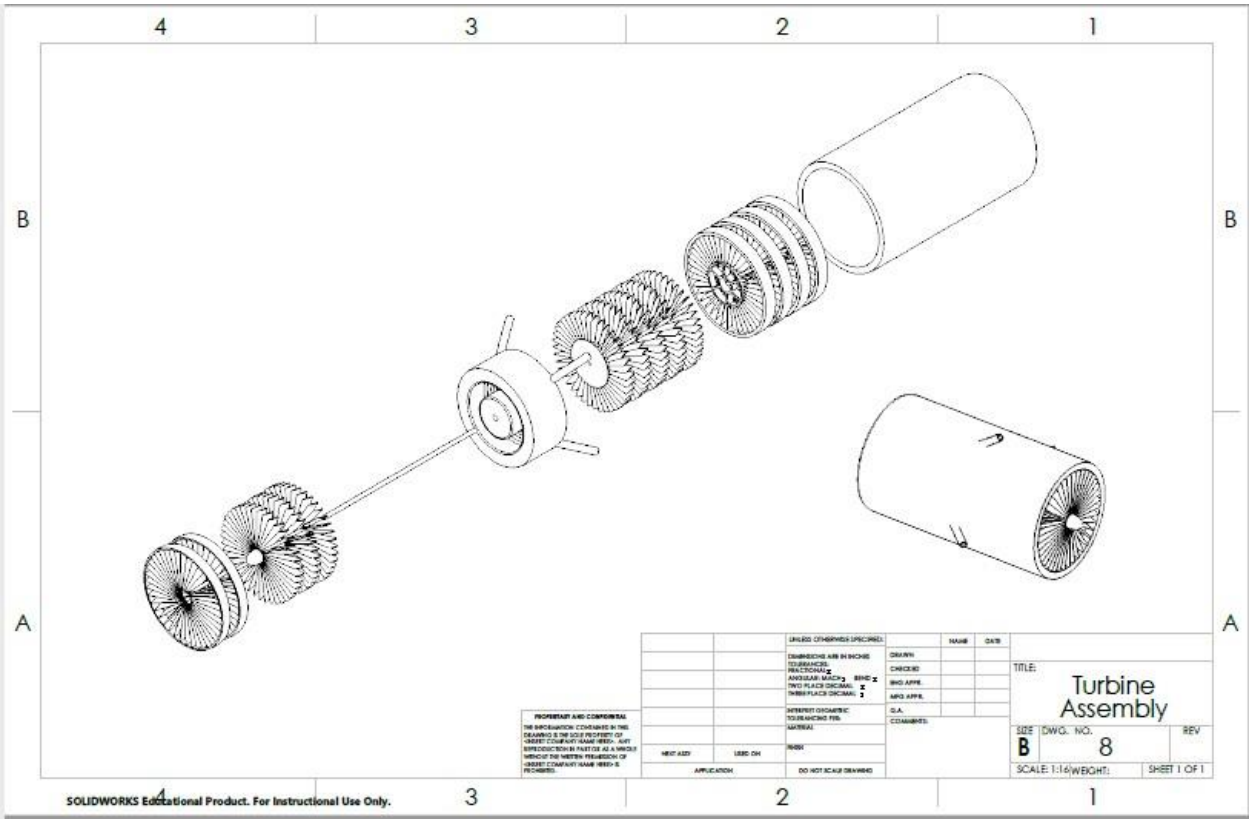

Figure 25: Final Assembly Drawing

As seen above, this design was very similar to the design chosen through the formal decision process. It uses a clear, outer casing of constant radius to allow for easy viewing of internal processes. While it is difficult to see in the above figure, it implements a variable hub radius to effectively compress air through the compressor section, and expand it through the turbine section; for a better look at this feature, refer to the detailed part drawings in Appendix C. In the middle "combustion chamber" section, heated compressed air is added to replace actual combustion. This is one area that was refined during the design process. In the initial concept shown in Figure 23, the compressed air was injected through a single port. This design would concentrate the flow in one location. To better distribute the flow throughout the cross section, the design was changed to have four ports evenly spaced throughout the combustion chamber. These ports are also aligned at an angle, to better direct the flow into the turbine section.

Another change to the design was the addition of stators, shown in blue, after rotor sections, shown in green. These were initially eliminated as the team thought they would make the design too difficult to manufacture. However, after more thorough research on compressor and turbine design, we determined that they would be necessary to better direct the flow through each stage, and to improve the efficiency of the model. All blade sections in the final design have an outer diameter of 16 centimeters, while the model has a total length of 30 centimeters.

5.2.1 Engineering Calculations

As noted earlier, each team member was assigned a subsystem of the design to analyze. These analyses were discussed in broad terms in the subsystem breakdown section above. A summary of the calculations performed for each subsystem is summarized below.

5.2.1.1 Compressor Calculations

A detailed description of the calculations performed for the compressor section can be seen in Appendix D. To summarize the calculations performed, first we calculated the Reynolds number for the inlet, assuming a turbulent flow. We estimated the sizes of the blades and the acrylic pipe that will contain everything. Using those assumptions, a Reynolds number was calculated across the blades and an airfoil shape was chosen to suit these numbers. The next step was to assume the speed at which the unit will rotate to start developing velocity triangles to figure out the angle of attack and geometric twist for the blades at each stage.

5.2.1.2 Combustion Chamber Calculations

The heated air flow for the combustion chamber was treated as an internal flow problem to calculate the amount of heat entering the system. The air flow comes from an air compressor running through a band heater for a simulated combustion chamber. The assumptions made for this design problem were the flow is fully developed, the flow will be treated as a laminar flow and the heat flux is constant. The final outcome for the design problem is the final temperature for the system. The Reynolds number for the air compressor was the first calculation made. Then the amount of heat flux can be calculated with the constant Nusselt number for a laminar flow. Then the mass flow rate can be calculated for the final temperature calculations. The amount of heat flux depends on the initial and final temperatures; however, the final temperature is the unknown so several iterations are needed so the numbers match.

5.2.1.3 Turbine Calculations

Similar to the compressor, the main parameter of interest in the turbine section is the angle of attack of the turbine blades. Currently, the team still has many unknowns which will affect the angle of attack of the turbine blades. In order to accommodate for these parameters, a MATLAB code was created to allow a user to input parameters such as volumetric flow rate, angular velocity, number of blade elements, and desired angle of attack. Using this information, the program outputs the pitch angle required at each blade location to maintain the desired angle of attack, as well as a plot representing the results. An example output, as well as a detailed breakdown of the MATLAB code and the calculations used within the MATLAB code, refer to Appendix F.

6 Proposed Design—First Semester

Most of the fundamental parts of the design, including the rotor and stator blades, will be 3D printed because they are a custom design. The components will be mounted on a shaft, with the rotors mounted on bearings to allow free rotation. The outer casing of the unit will be a clear acrylic tubing that will allow students to see through to each stage. Ports will be drilled in various locations along the model to allow for several key components. The most important of these are the ports outside of the combustion chamber for compressed air. As noted earlier, heated compressed air will be injected at this stage to simulate the combustion process. This will be accomplished using a Porter Cable air compressor and tank, and a 100-Watt band heater wrapped around the air hose between the air compressor and combustion chamber.

As previously discussed, one of the vital engineering requirements was temperature and pressure measurement, derived from the client's request for interactivity. To thoroughly analyze the thermodynamic Brayton Cycle, four temperature and pressure measurements are needed: one at the entry to the compressor, a second at the entry to the combustion chamber, a third at the exit of the combustion chamber, and a fourth at the exit of the turbine. Ideally, the team would utilize separate measurement instruments for each of the four locations. However, due to a limited budget of just $500, a compromise had to be made in this area. Rather than using four pressure transducers, a single pressure transducer was to be used to monitor all four locations. We intended to design a valve system to allow each port to connect to the same transducer; the

measurement location will be changed by opening the valve for the desired port and closing the other three. The pressure transducer was to be mated to a National Instruments NI-6009 14-bit data acquisition (DAQ) device for data acquisition, provided by the client, Professor David Willy.

Temperature measurement was also compromised slightly due to budget constraints. Thermocouples are inexpensive, so one J-Type thermocouple was specified at each of the locations of interest. However, the budget only allows for a single-input temperature measurement DAQ device, the National Instruments USB-TC01. Each thermocouple had its own male adapter, to allow the user to easily switch between measurements. Both DAQ devices are controlled by LabVIEW Virtual Instrument (VI) software, which allows for data collection and manipulation. Table 6 shows a complete Bill of Materials for the final design.

Table 6: Bill of Materials

Bill of Materials						
Item	**Quantity**	**Cost per unit**	**Manufacturer**	**Item #**	**Vendor**	**Hyperlink**
Acrylic Tubing	1 ft	$13.43	U.S. Plasic Corp	44550	U.S. Plastic Corp	https://goo.gl/rmKMEm
3D Printed Compressor Blades	255 g	$25.50	MakerBot	N/A	NAU Cline Library	See Part Drawing
3D Printed Compressor Stator Blades	292 g	$29.20	MakerBot	N/A	NAU Cline Library	See Part Drawing
3D Printed Turbine Blades	152 g	$15.20	MakerBot	N/A	NAU Cline Library	See Part Drawing
3D Printed Turbine Stator Blades	213 g	$21.30	MakerBot	N/A	NAU Cline Library	See Part Drawing
3D Printed Combustion Chamber	208 g	$20.80	MakerBot	N/A	NAU Cline Library	See Part Drawing
Ceramic 608 Bearings	2	$8.99	Acer	SK8	Acer Racing	https://goo.gl/5BpiMh
Air compressor with tank	1	$89.00	Porter Cable	C2002	CPO Commerce	https://goo.gl/KRQu8p
Band Heater	1	$28.50	Tempco	NHL00100	Grainger	https://goo.gl/WnqnU8
J Type Thermocouple Wire	7.62 m	$0.60	TIP Industries	TIPWRJ008	TIP Industries	https://goo.gl/PiFj3X
Thermocouple Connectors	1	$3.05	Omega	OST-U-M	Omega	https://goo.gl/bAjo9v
Thermocouple DAQ	1	$107.00	National Instruments	USB-TC01	National Instruments	https://goo.gl/U5soAU
Pressure Transduser	1	$49.00	Transducers Direct	TDH30BG025003B004	Transducers Direct	https://goo.gl/ZAUC21
Pressure Transduser DAQ	1	$250.00	National Instruments	USB-6009	National Instruments	https://goo.gl/xaw9sP
	Total:	**$661.57**				

At this stage, the team was still working on finalizing the design. In order to stay on schedule, the team created a simplified agenda outlining the remaining major milestones and the approximate date by which they should be completed. This schedule is summarized in Table 7.

Table 7: Implementation Schedule

Milestone	Target completion date
Perform testing with Thermo 1B team device	September 9
Finalize design details	September 16
Order remaining parts	September 19
Complete 3D printing	October 7
Complete testing procedures	November 3
UGRADS Poster	November 5
Final Report/CAD Package	December 3

7 Implementation

All the work discussed thus far was completed during the first semester of the project. After taking a break for the summer, the team resumed work in the fall semester. The team's initial plan for the second semester is discussed in section 7.1, while section 7.2 details how implementation has actually taken place thus far.

7.1 Manufacturing

Most of the manufacturing necessary for this project will be 3D printing. For the device to function properly, it is important that the 3D printed parts fit together with close tolerances. To ensure this, the team will first print a test ring to compare with the inner diameter of the tubing that will be used for the outer casing. Once the team knows the correct dimensions the CAD model will be updated and sent to the MakerLab for the first iterations of the blades. These blades will be used for the first testing of the system to ensure size and functionality of the model. After the team knows the blades are fully functional, the CAD drawing will be sent to the RapidLab for a higher print quality.

The only other custom manufacturing necessary will be the rotating shaft to which the blades will be attached. The diameter of the shaft will be determined by the bearings. The team selected 608z ball bearings because they are common in many products and are easy to find in many variations. Ungreased, ceramic bearings will be the best option for this design because they have minimal friction. These bearings are designed to fit on a shaft with an 8-millimeter nominal diameter. Finding an 8-millimeter shaft might prove difficult and expensive, so finding a shaft that is close in size and machining it to the desired size will be the best option. One of the team members has access to and experience using a lathe, so the team does not have to outsource machining for the shaft.

The majority of the remaining parts will be purchased online or off the shelf. As noted earlier, the 3D printed blades and shaft will be mounted in acrylic tubing, which will be ordered online. This assembly will be mounted to a cart to allow for easy transportation into and out of the classroom. The cart will contain all other equipment necessary to run this experiment. The most important aspect of this will be the data collection system, which utilizes thermocouples and pressure transducers to measure temperature and pressure. The client requested that these variables be measured at four points: the compressor inlet and outlet, and the turbine inlet and outlet.

At the beginning of the semester the team learned that the previous capstone team purchased two pressure transducers that were available to use. Thus, the team intends to design a manifold type system to allow four pressure measurements to be taken using just two transducers. Each manifold will have two "branches"

that will go to the separate points, each branch being controlled by a valve that will allow switching between different points.

Additionally, the team intends to purchase the cart mentioned above, thermocouple wires, connectors, and a data acquisition system. All the components have been sourced and will be ordered online or purchased locally in Flagstaff. Many of these components were changed since last semester. An updated Bill of Materials is presented for reference in Appendix G.

Finally, the team also needs to design a simple LabVIEW program to collect the temperature and pressure measurements. This will be controlled by a laptop which can be mounted on the cart next to the model turbojet. The client requested that this program also be able to visually display the collected data, preferably through graphs. The team intends to meet with him to finalize the details of this program.

Once 3D printing is finished and all necessary components arrive, the team should be able to assemble the device relatively quickly. However, it is likely many variations will need to be made once the device is assembled and tested. The updated implementation schedule is presented in Table 8 but is still expected to change.

Table 8: Updated Implementation Schedule

Milestone	Target completion date
Perform testing with Thermo 1B team device	September 9
Finalize design details	September 16
Order remaining parts	September 19
Complete 3D printing	October 24
Device manufacturing/assembly	October 28
Complete testing procedures	November 11
Iterate and redesign	November 16
UGRADS poster	November 30
Operation and Assembly Manual	November 30
Final Report/CAD Package	December 5

7.2 Design Changes

This semester, the team began by testing the prior iteration of the design created by the previous capstone team. Based on this testing, we decided to make several changes to our design. The most significant change was to reduce the outer casing diameter from 6 inches to 4.5 inches. In our testing, we noted that the compressed air tank selected for the design ran empty much too quickly. Changing the diameter decreases the mass flow rate and rotational inertia of the blades, which should allow for a longer run time. It also decreases the cost of 3D printing and acrylic tubing.

The testing also revealed that the system operating temperatures could get quite high, which made the team decide to change the thermocouple type from basic J-type to insulated K-type to increase the measurable temperature range. Then the team also decided to decrease the number of stages in the compressor and the turbine. With this design change, the team can save on cost, make more space on the cart, and reduce the rotating mass.

The team also reviewed the first design and made a few changes that should further improve performance. The previous iteration of the design utilized a combustion chamber with four inlets. This was redesigned to accept one inlet from a compressed air source, and then diffuse the air in a manner modelled after a Dyson fan. Having only one air inlet will simplify manufacturing, and the new diffuser design will distribute the heated air more efficiently. An updated CAD model is shown below in Figure 26

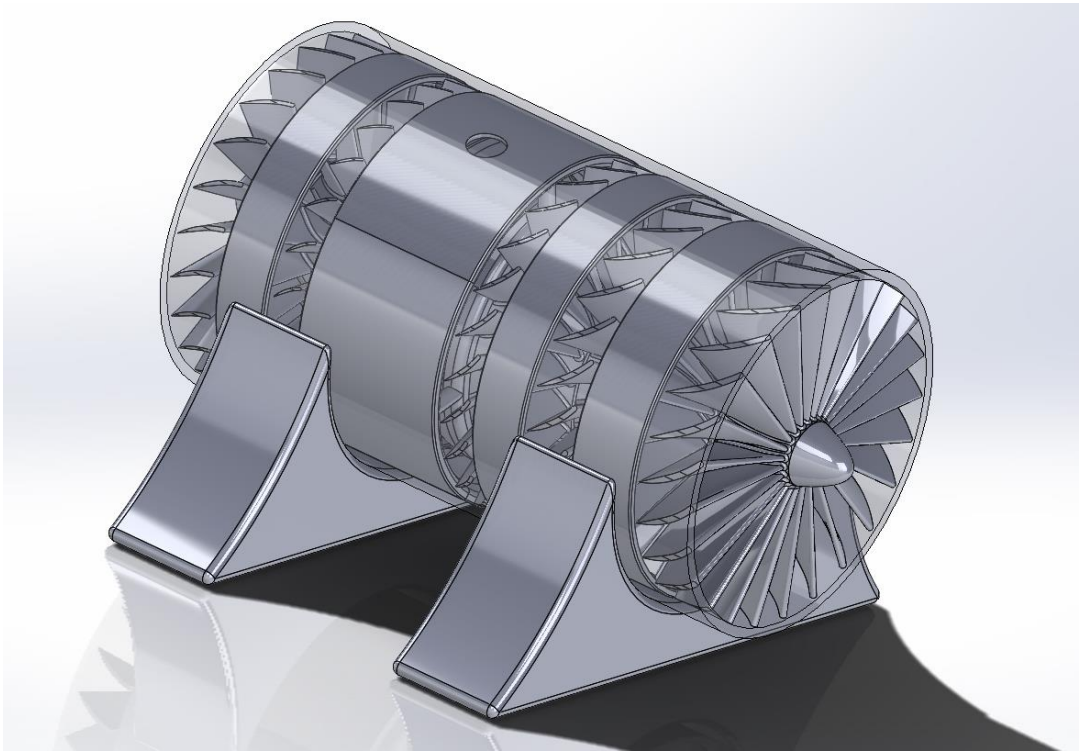

Figure 26: Current CAD model

.

The first step of manufacturing was ordering all the parts needed from the respective vendors. Once the premade items were on the way, the test piece previously mentioned in the manufacturing plan was designed and printed. This fixture tested blade and stator fitment, shaft fitment, and bearing fitment, and is shown below in Figure 27. While difficult to see in the figure, the outside diameter has steps to test different blade diameter fitments in the acrylic tubing. The smaller circles on the inside test bearing and shaft fitment.

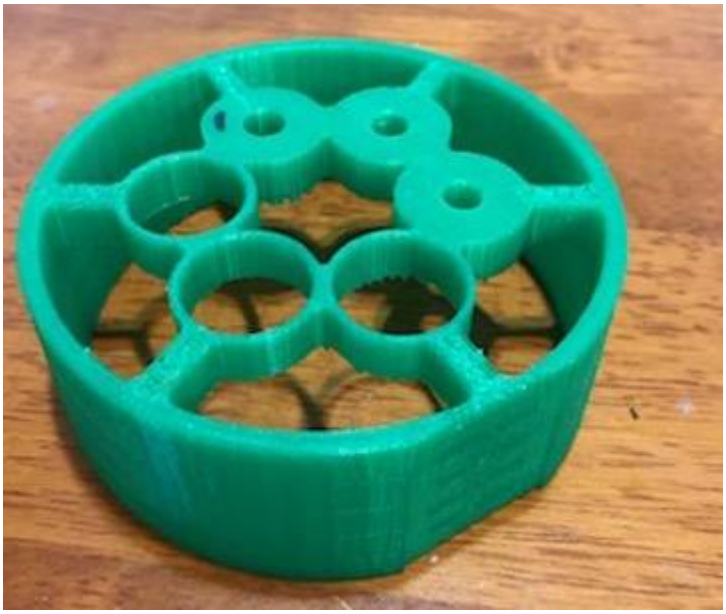

Figure 27: Blade Fitment Test Fixture

Unfortunately, after testing this component in the purchased acrylic tube, the team found it was too small, so another had to be printed with larger outer diameter sizes. The newer version had the correct sizing, which allowed the team to determine the correct sizes for the stators and blades. Based on these findings, slight adjustments were made to the blade and stator diameters in the CAD model to ensure a tight fit. The updated CAD models were sent to the NAU MakerLab and are currently in production. Two stator sections have finished printing, and are shown in Figures 28 and 29.

Figure 28: First Stator Section

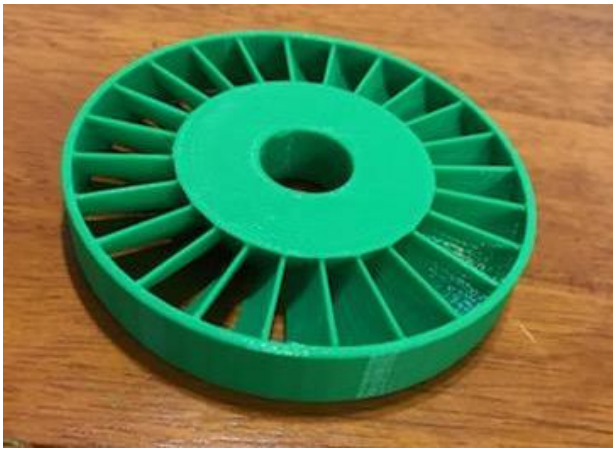

Figure 29: Second Stator Section

The team also had to make a slight adjustment to the combustion chamber design to accommodate 3D printing. The new design has a closed has a very thin, internal slit along its circumference to evenly distribute the air. This presents a challenge as the support material required during 3D printing would be very difficult to remove. For testing purposes, the team decided to cut the combustion chamber into four pieces to facilitate removal of the support material. This is shown in Figures 30 and 31 below. However, for the final version, the team intends to print this in the RapidLab on a 3D printer that uses dissolvable support material, meaning it can be printed in one piece.

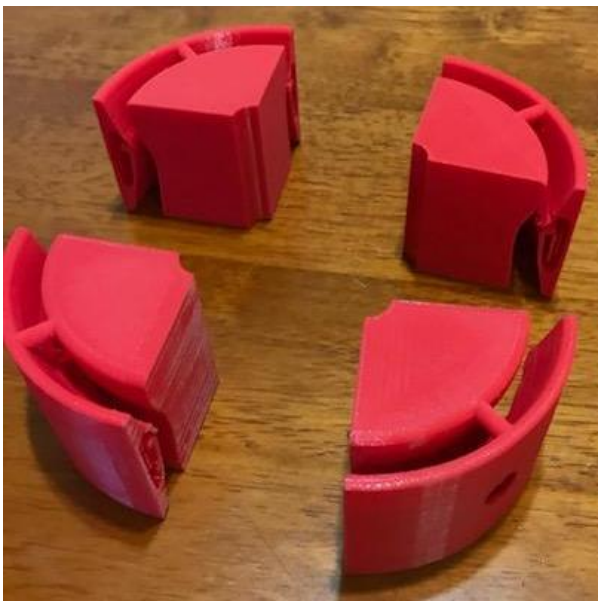

Figure 30: Combustion Chamber Cut Sections

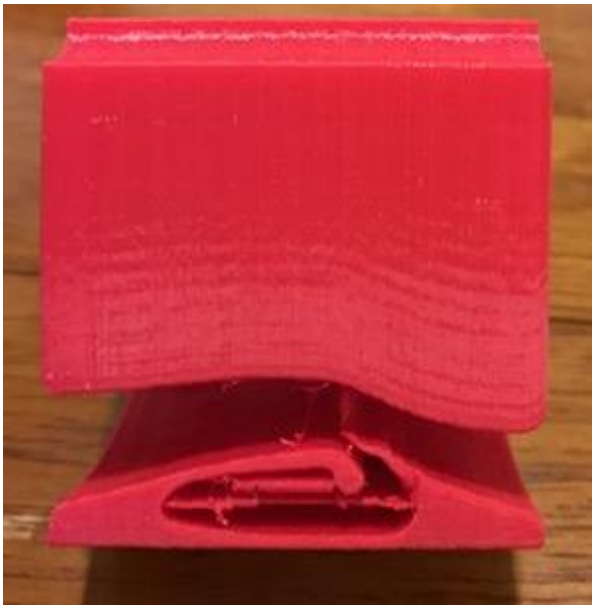

Figure 31: Support Material in Diffuser

The team underestimated how long the prototype 3D printing would take, which has slowed progress, as assembly cannot occur without the blades. However, the team has worked on a few other subsystems in the meantime. First, the purchased shaft was machined from ⅜ in to 8mm for tight fitment with the bearings. This is shown below in Figure 32.

Figure 32: Shaft Machining

The team also created the prototype for the pressure manifold system described in the previous section using brass fittings purchased from Home Depot. This design will need to be modified slightly to fit properly on the final system. However, Figure 33 shows a representation of one-half of the system to demonstrate how it will work.

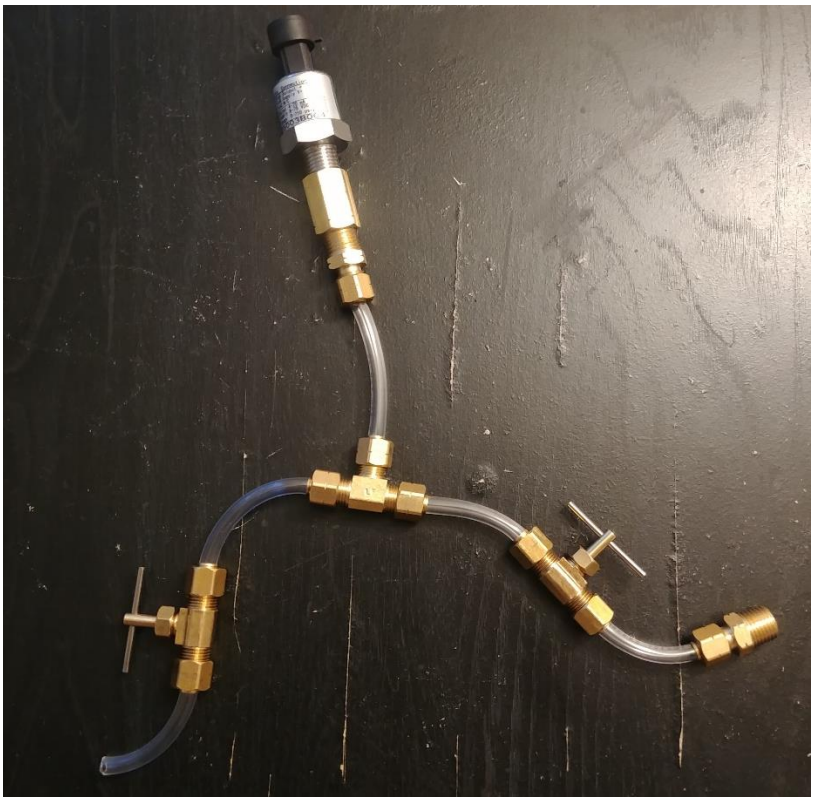

Figure 33: Pressure Measurement Manifold

Finally, the team assembled the utility cart that will be the base of the design. Two changes were made to the cart. First, we decided to invert the top tray of the cart to obtain a flat surface to mount the turbojet model and data acquisition equipment. This will also allow wiring to be hidden underneath, improving safety and aesthetics. We also decided to paint the cart in NAU colors. The painted and assembled cart is shown in Figure 34.

Figure 34: Painted Cart

The team is currently reviewing the compressed air system and may potentially change this in the future. As noted previously, we found that the current air compressor and tank empties too quickly. While our design changes should extend the runtime, a larger tank would still be desirable. The team is considering several options, such as connecting a second tank, or eliminating the air compressor and mounting a much larger air tank which would need to be charged outside the classroom before demonstration. This decision will be finalized after a meeting with our client next week.

References

[1] K. Hunecke, "Engine Classification," in *Jet Engines: Fundamentals of Theory, Design, and Operation,* Ramsbury, England: The Crowood Press Ltd, 1997, ch. 1, sec. 1.2, pp. 3-10.

[2] *The Market For Missle/Drone/UAV Engines* [Online]. Available: http://www.forecastinternational.com/samples/F655_CompleteSample.pdf

[3] *MiniLab Gas Turbine Lab* [Online]. Available: http://www.turbinetechnologies.com/educational-labproducts/turbojet-engine-lab

[4] *Wren 50 Turbo Prop* [Online]. Available: http://www.wrenpowersystems.com/helitp.html.

[5] *RC Turboprop Model Jet Engines Explained* [Online]. Available: https://www.rc-airplanessimplified.com/model-jet-engines.html.

[6] N. Hall (2015, May 5). *Compressors* [Online]. Available: https://www.grc.nasa.gov/www/k12/airplane/compress.html.

[7] D. Newman (2003, Mar.). *Turbines and Compressors* [Online]. Available: http://ffden-2.phys.uaf.edu/212_fall2003.web.dir/Oliver_Fleshman/turbinesandcompressors.html.

[8] J. Escobar. (2003, May 1). *Turbine Engine Compressor Sections. Basic theory and operation* [Online]. Available: http://www.aviationpros.com/article/10387158/turbine-engine-compressorsections-basic-theory-and-operation

[9] S. Farokhi, "Axial Compressor Aerodynamics" in *Aircraft Propulsion*, 2nd ed., Chichester, United Kingdom: John Wiley & Sons Ltd, 2014, ch. 8, sec. 8.3, pp. 527-529.

[10] Q. Nagpurwala, *Design of Gas Turbine Combustors,* Bengaluru: M.S. Ramaiah School of Advance Studies.

[11] K. Hunecke, "Engine Classification," in *Jet Engines: Fundamentals of Theory, Design, and Operation,* Ramsbury, England: The Crowood Press Ltd, 1997, ch 5, sec 5.1, ppg 125-126

[12] K. Hunecke, "Turbine," in *Jet Engines: Fundamentals of Theory, Design, and Operation,* Ramsbury, England: The Crowood Press Ltd, 1997, ch. 6, sec. 6.1, pp. 137-145.

[13] *Jet Engine Design: The Turbine* [Online]. Available: http://aerospaceengineeringblog.com/jetengine-turbine/

[14] *Stator of Turbine* [Online]. Available: http://www.ekolenergo.cz/aktualitygb.html

[15] *Types of Turbines* [Online]. Available: http://www.idc-online.com/control/Types_of_Turbines.pdf

[16] S. Farokhi, "Aerothermo-dynamics of Gas Turbines," in *Aircraft Propulsion*, 2nd ed., Chichester, United Kingdom: John Wiley & Sons Ltd, 2014, ch. 10, sec. 10.2, pp. 685-713.

[17] *Angle of Attack* [Online]. Available: https://www.skybrary.aero/index.php/Angle_of_Attack.

[18] *Intex Quick-Fill Rechargeable Air Pump, 110-120 Volt, Max. Air Flow 21.2CFM* [Online]. Available: https://goo.gl/6HC12U

[19] *155 MPH 200 CFM 6 Amp Electric Handheld Leaf Blower Blue* [Online]. Available: https://goo.gl/JMt87v

[20] Cambered plate C=14% T=5% R=0.96 (cp-140-050-gn) [Online]. Available: http://airfoiltools.com/airfoil/details?airfoil=cp-140-050-gn

[21] W.W. Bathie. Fundamentals of Gas Turbines. New York, NY: John Wiley & Sons, 1996, pp. 248254.

Appendices

Appendix A: Concept Sketches

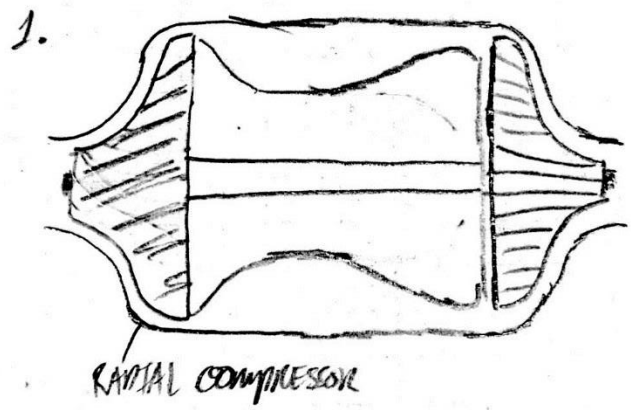

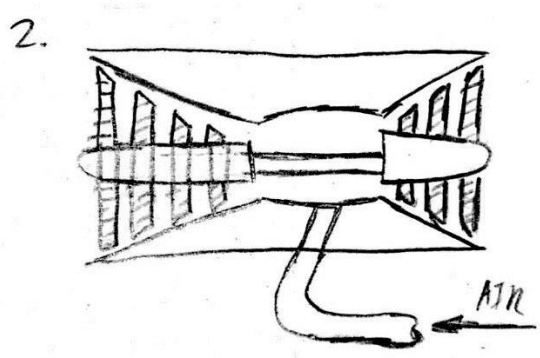

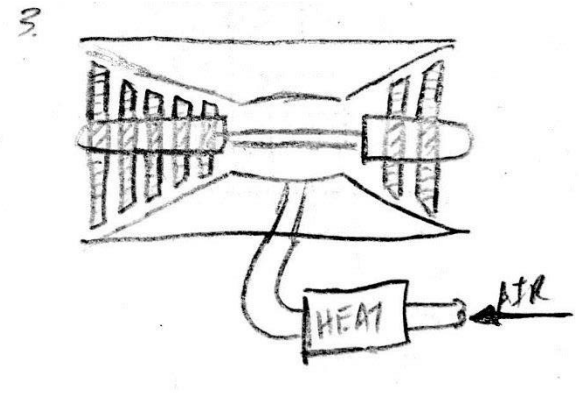

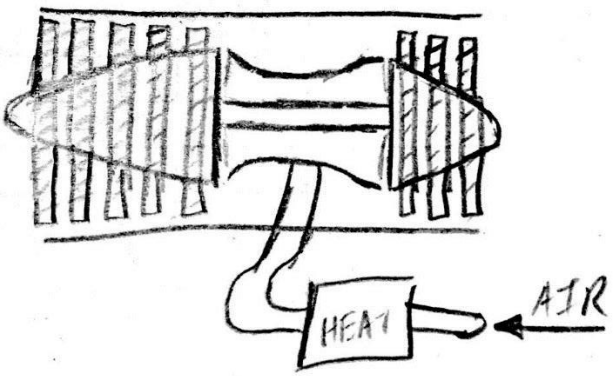

5.

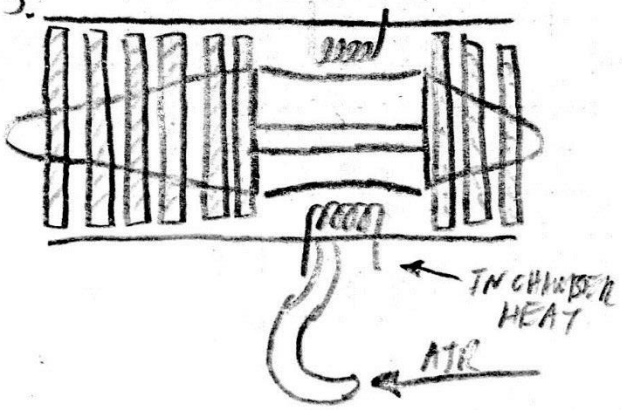

6.

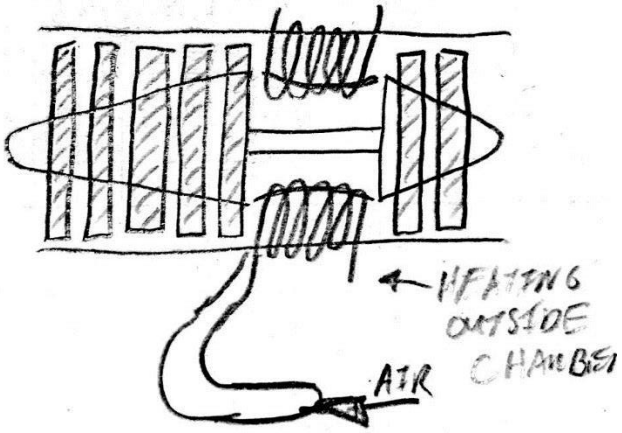

7.

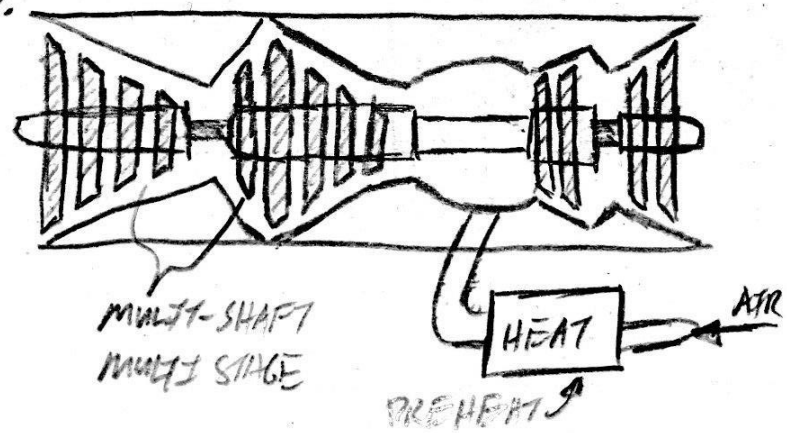
MULTI-SHAFT
MULTI STAGE
HEAT
AIR
PREHEAT

8.

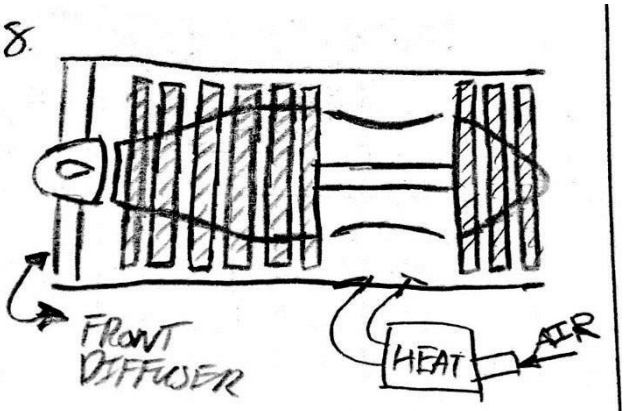
FRONT
DIFFUSER
HEAT
AIR

9.

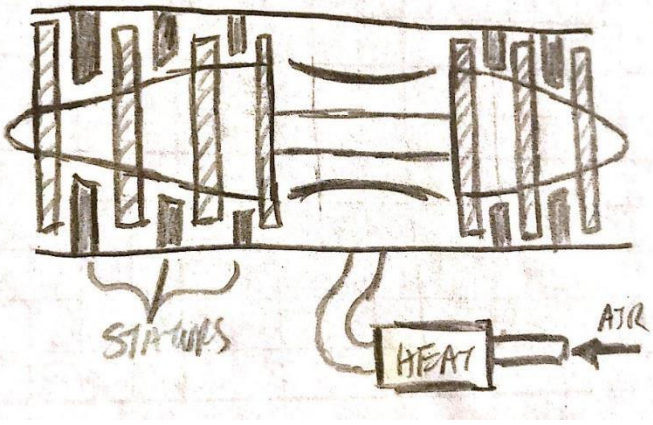
STATORS
HEAT
AIR

10.

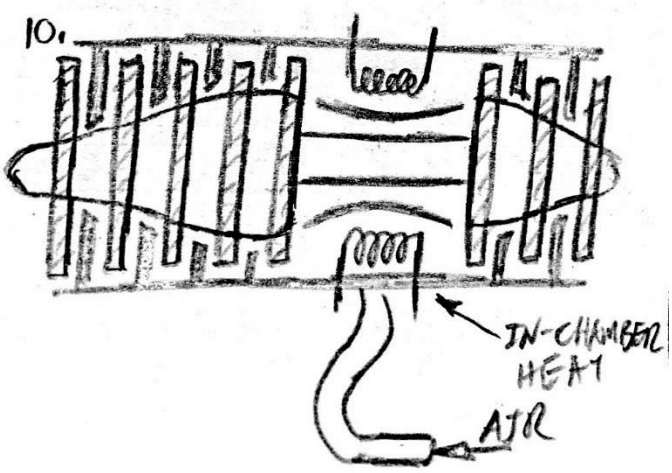
IN-CHAMBER
HEAT
AIR

11.

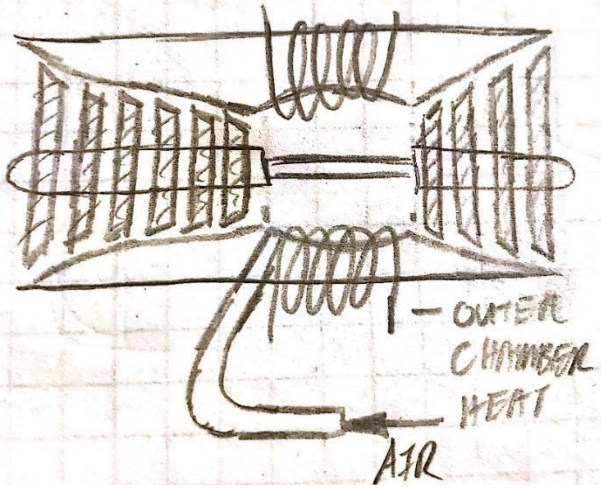
OUTER
CHAMBER
HEAT
AIR

12.

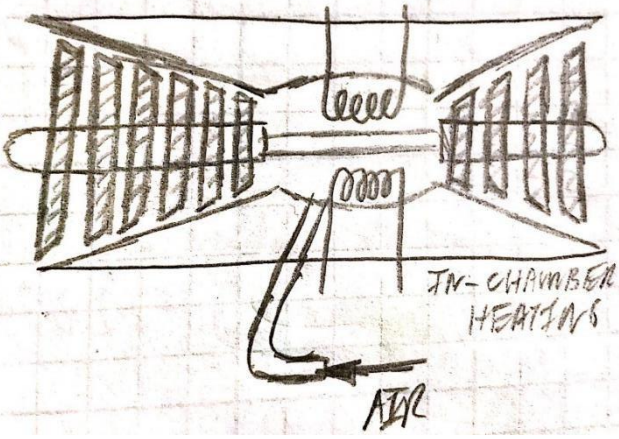
IN-CHAMBER
HEATING
AIR

13.

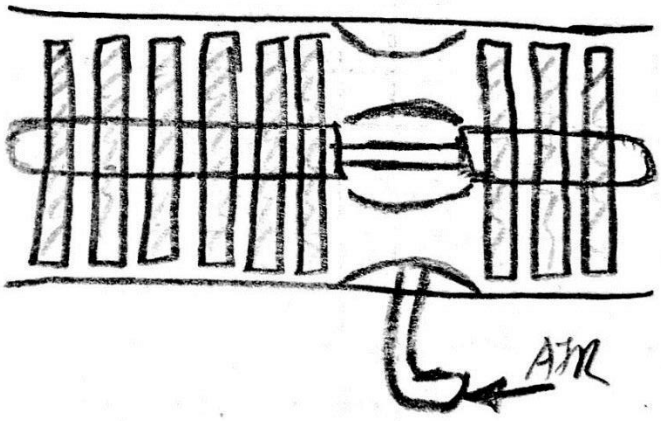

14.

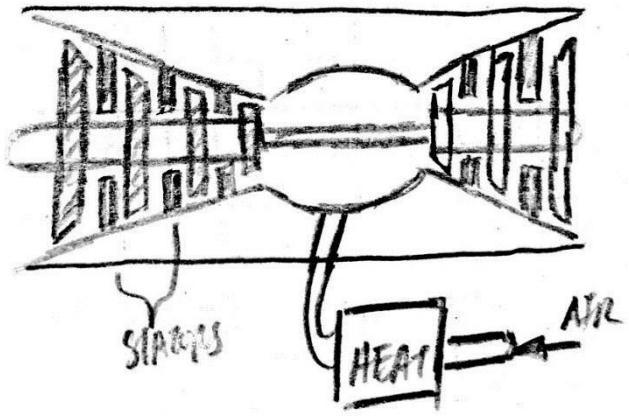

15.

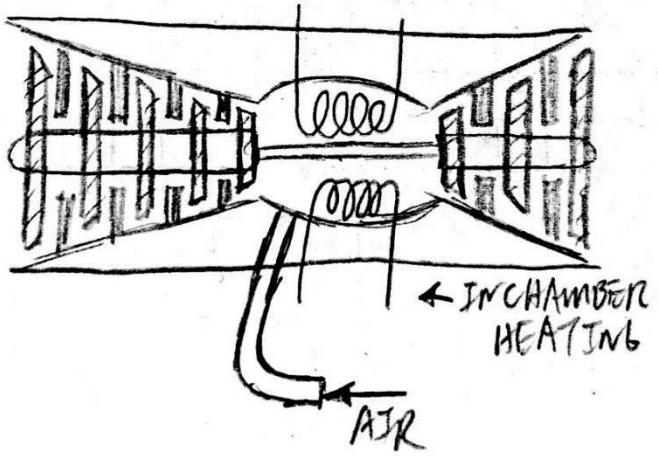

DESIGN 9

STATOR COMP. + TURBINE W/PREHEAT, CONSTANT OUTER DIAM.

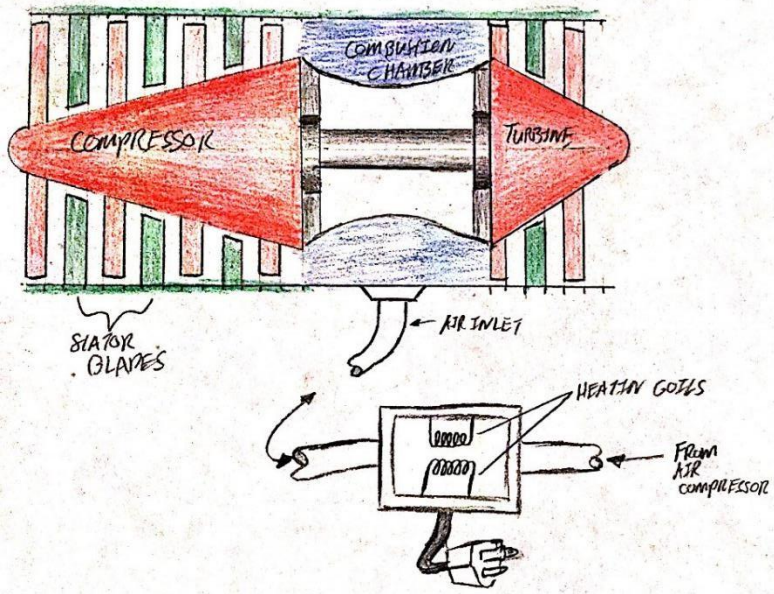

DESIGN 11

STATORLESS COMPRESSOR & TURBINE, W/PREHEAT, NON-CONSTANT DIAMETER

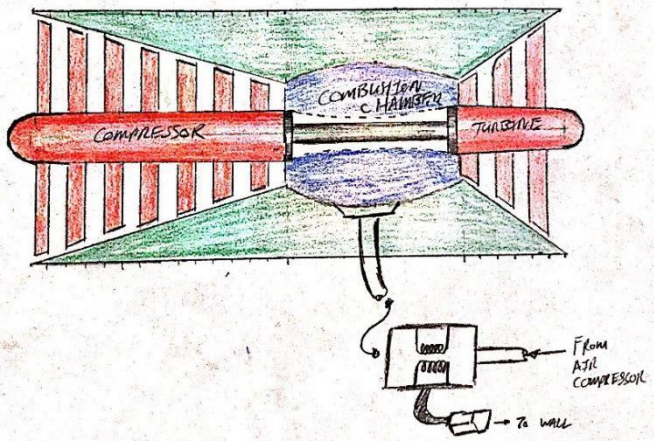

DESIGN 13

CONSTANT INER & OUTER DIAM, STATORLESS, NO HEAT

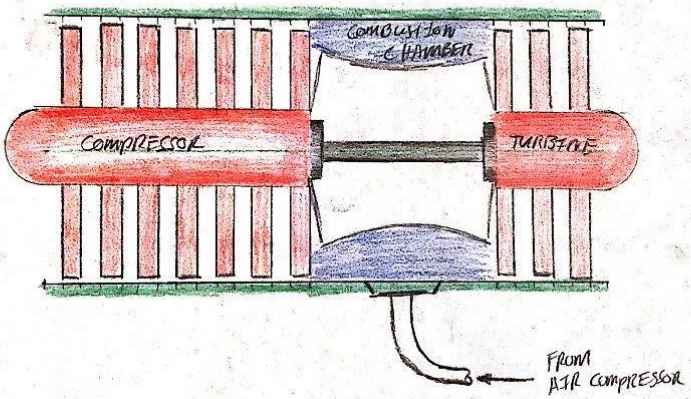

DESIGN 14

STATORLESS, CONST. OUTER DIAM, PREHEAT

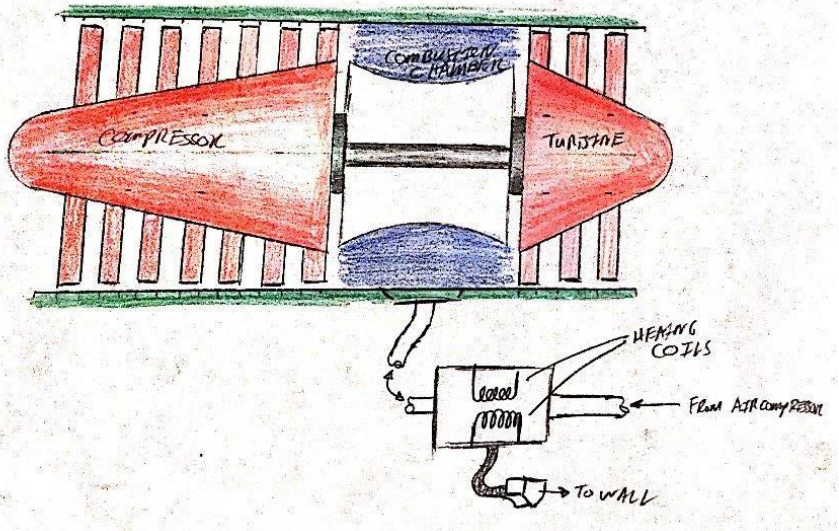

Appendix B: Pugh Chart

	1	2	3	4	5	6	7	8	9	10	11	12	13	14	15
Portable	-	s	s	s	s	s	s	s	s	s	s	s		-	s
Interactive	-	-	-	+	+	+	-	s	+	-	-	s		s	s
Educational	-	-	+	+	+	+	+	s	+	-	s	s	D	+	s
Durable	+	-	-	s	-	-	-	-	s	-	+	+		s	s
Reliable	-	s	-	-	-	-	-	-	-	-	s	s		-	-
Fit in 2x3 foot perimeter	s	s	s	s	s	s	s	s	s	s	s	s	A	s	s
Total weight < 100lbs	-	s	s	s	s	s	s	s	s	s	s	s		s	s
Demo < 15 minutes	s	s	-	-	-	-	-	-	-	-	-	-		-	-
Visability	-	-	-	s	s	s	-	-	s	-	-	-	T	-	s
120v AC, 60Hz, and/or compressed air	-	s	s	s	s	s	s	s	s	s	s	s		s	s
Minimize exposure	-	s	s	s	s	s	s	s	s	s	s	s		s	s
Feasibility	-	-	-	-	-	-	-	s	-	-	s	-		-	s
Efficiency	-	+	+	+	+	+	+	+	+	+	s	s	U	+	+
Cost	-	-	-	-	-	-	-	-	-	-	-	-		-	-
Total -	11	6	7	4	5	5	7	5	4	8	4	4		6	3
Total +	1	1	2	3	3	3	2	1	3	1	1	1	M	2	1
Total s	2	7	5	7	6	6	5	8	7	5	9	9		6	10

Figure B1: Pugh Chart

Appendix C: Part Drawings

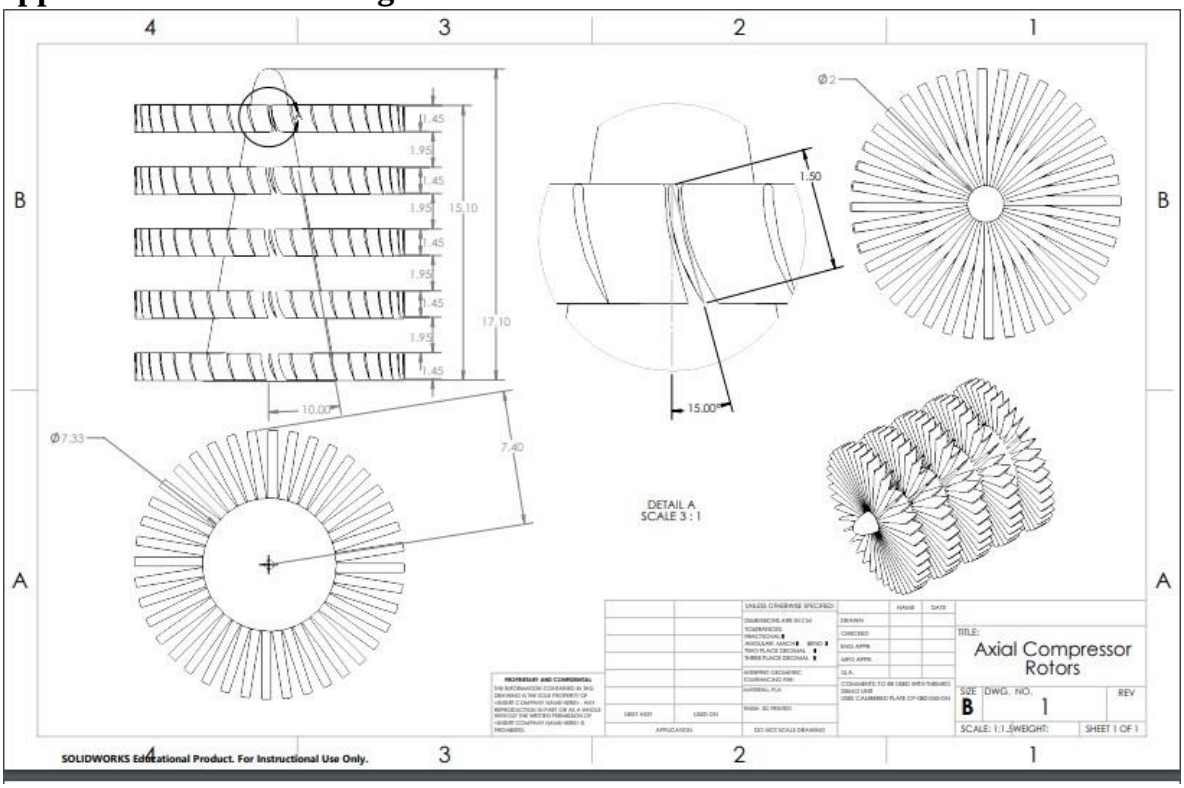

Figure C1: Compressor Rotors

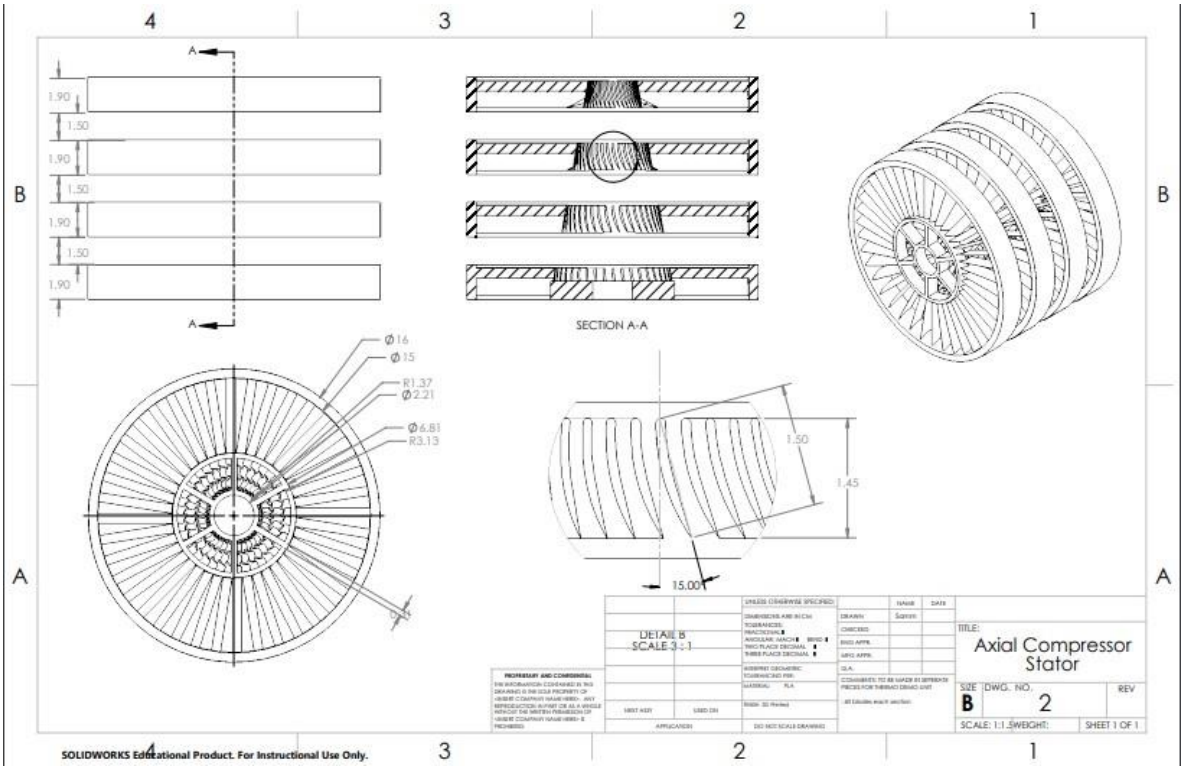

Figure C2: Compressor Stators

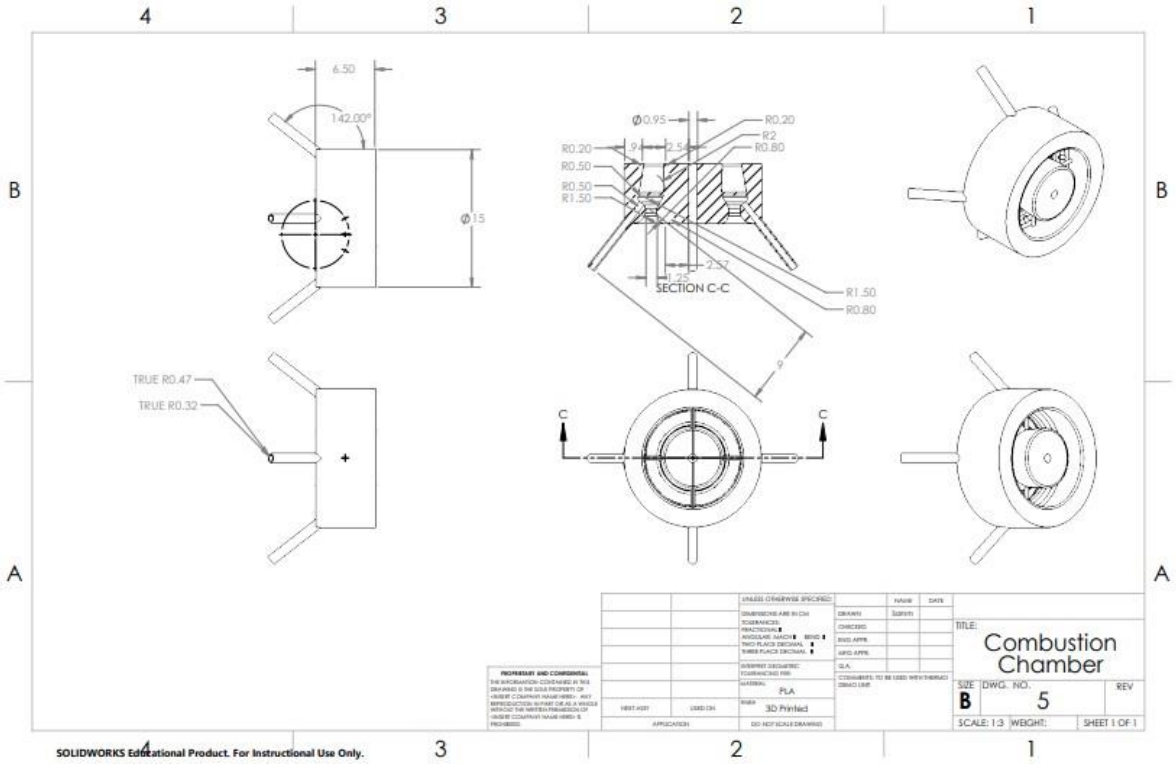

Figure C3: Combustion Chamber

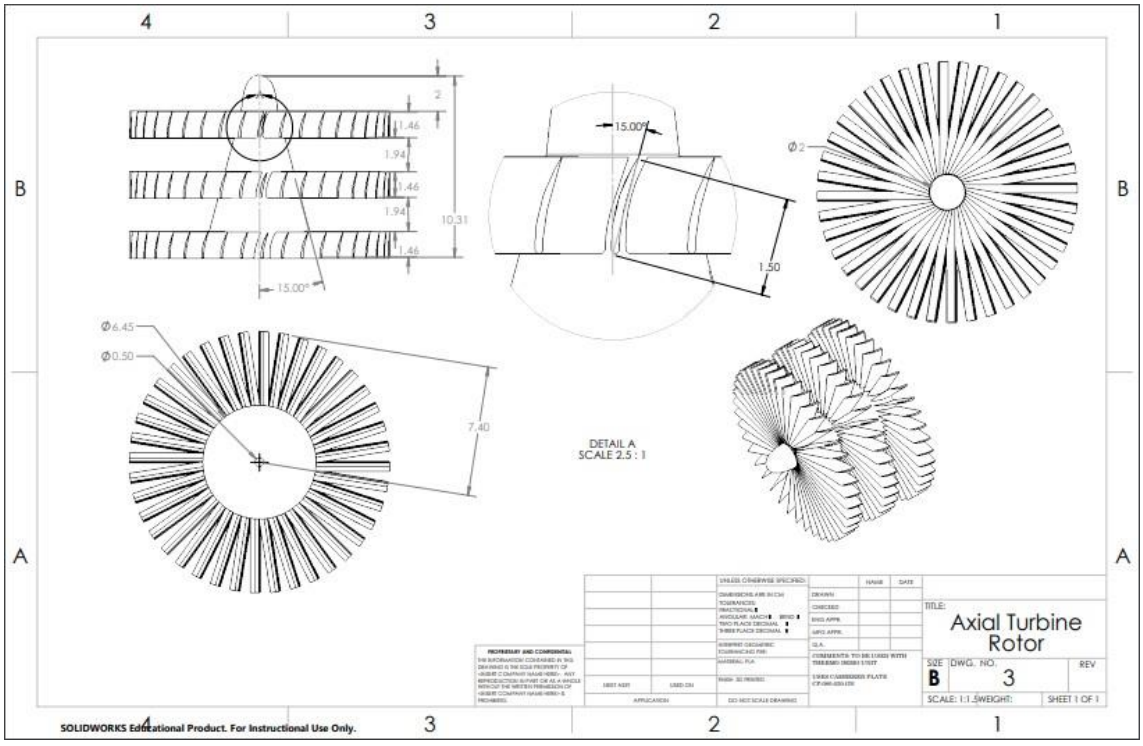

Figure C4: Turbine Rotors

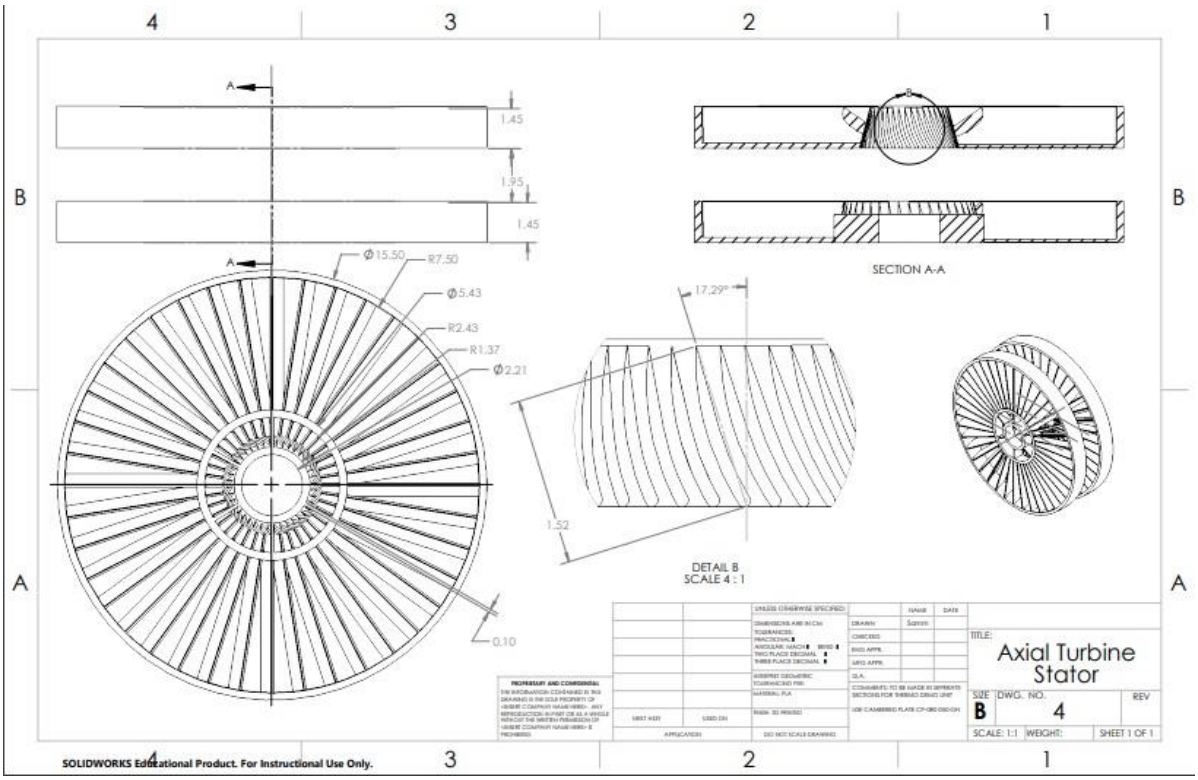

Figure C5: Turbine Stators

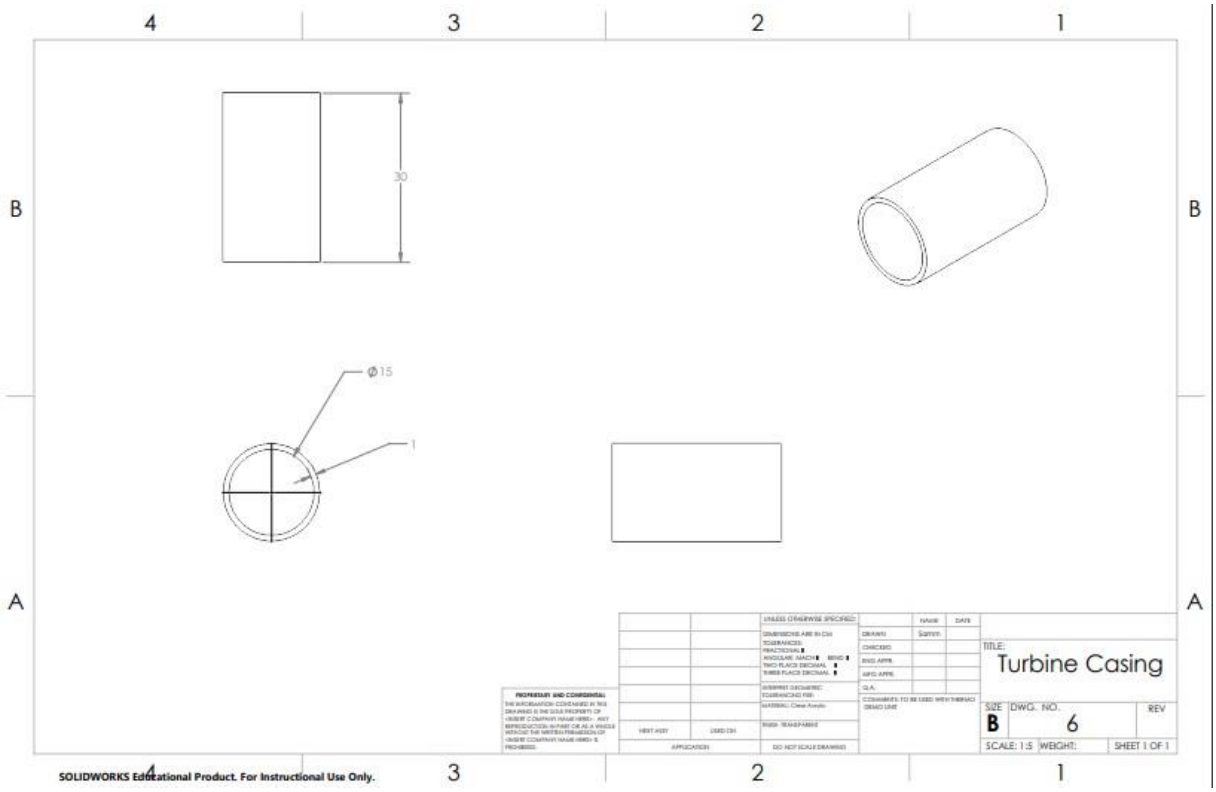

Figure C6: Outer Housing

Appendix D: Engineering Calculations—Compressor

The most important part of the calculations was the assumptions we were going to make do we could continue forward. We assumed a turbulent flow at the inlet to ensure an even velocity profile at the inlet, and because everyday jet engines experience turbulent flow at the inlet as well. Based on that, the Reynolds number for a turbulent internal flow must be above 4000: we assumed an inlet Reynold's number of at least 4500. From that we were able to find an inlet velocity using equation D1 below.

$$v_{inlet} = Re^{inlet} * \mu / \rho D \qquad (D1)$$

Re_{inlet} is the Reynold's number at the inlet, μ is the dynamic viscosity of the fluid, in this case it is air, ρ is the density of the fluid, and D is the diameter of the inlet. Assuming standard temperature and pressure, and an inlet size of 15 centimeters the minimum inlet velocity of .4510 m/s was calculated. That is almost exactly 1 mile per hour. Seeing as how the unit will be stationary for demonstration and that the inlet velocity is very low, the unit should be able to operate in a room with no inlet velocity aside from the suction it will create as it operates.

To start analyzing the blades, a 2cm hub radius was assumed at the first stage of the compressor, yielding a blade length of 6.4 cm leaving a 1 mm clearance between the blade and inner wall of the acrylic pipe. Using this information the Reynold's number at the blades was calculated from equation D2 below. .

$$Re_{blade} = \rho v_{inlet} L / \mu \qquad (D2)$$

T airfoil. The chord is the length of the line connecting the leading and trailing edges of an airfoil [3]. I assumed this to be 1.5 cm because it seemed like a reasonable length, and most likely will be adjusted later. The Reynold's number I calculated at the blades was 450. These numbers were much lower than I saw on recommended Reynold's number for the airfoil on *airfoiltools.com*, but they will still work for initial calculations.

The next step was to assume a speed that the model will rotate at. From our initial research about the project I had found the Wren 50 model engine [4]. This engine uses real combustion and has similar dimensions to our design. The engine idles at 55,000 rpm and because our design is slightly larger I used that speed in my calculations. I converted that speed to radians per second and used that value to find the angular velocity of the blades using equation D3 below.

$$U_1 = r * \omega \qquad (D3)$$

The radius of the blades is represented by r, and omega is the speed in radians per second of the blades. Figure 2 below shows the structure of the velocity triangles and how they will be solved

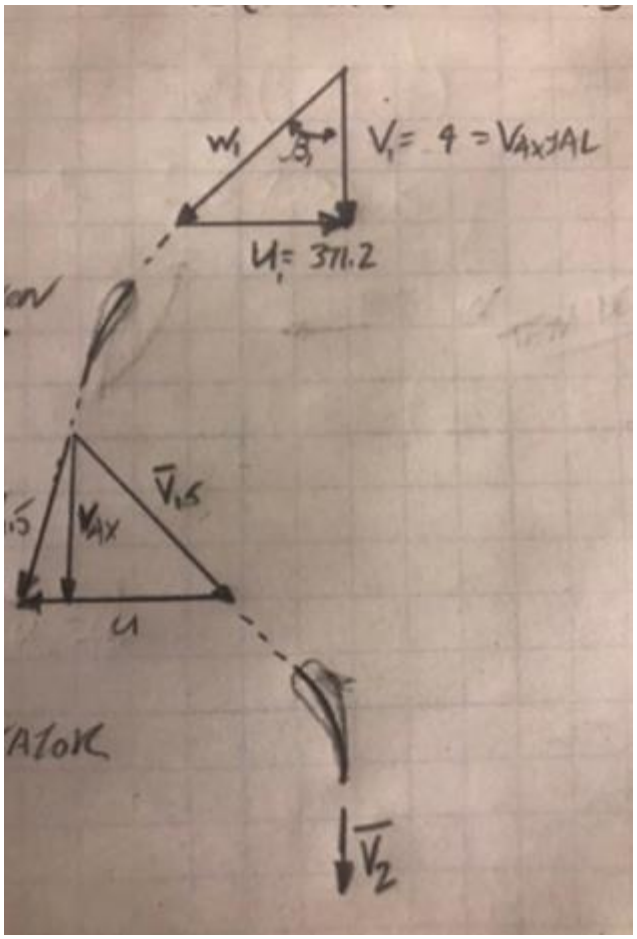

Figure D1: *velocity triangle and blade diagram*

The lower blade is the stator, and the upper triangle is the rotor. Both of these together make up stage 1. The equations and processes for finding β_1, $\beta_{1.5}$, $\alpha_{1.5}$, and v_2 can be seen below in figures 3 and 4.

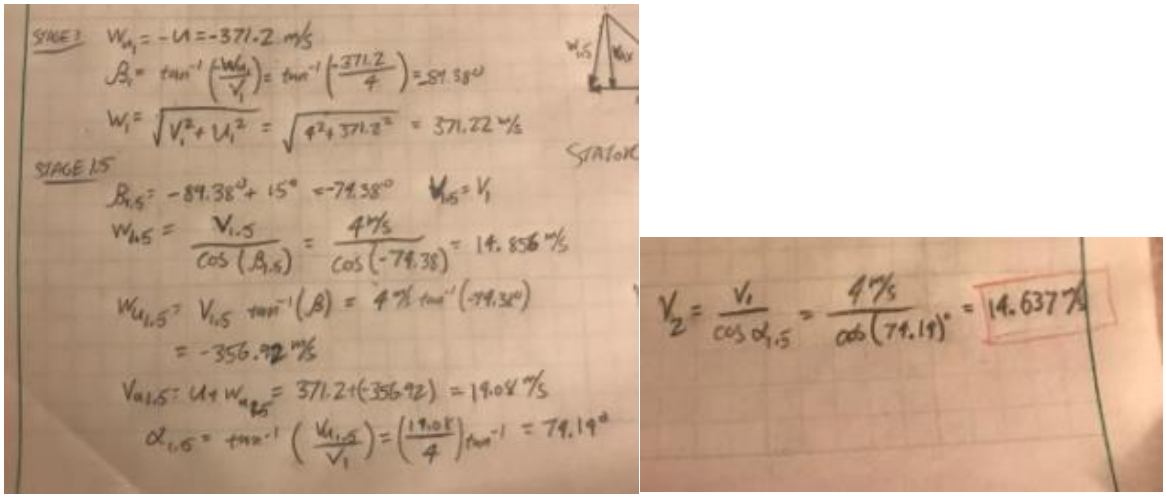

Figure 3,4: *velocity diagram calculations*

Appendix E: Engineering Calculations—Combustion Chamber

The following equations were used in the analysis of the combustion chamber:

$$Re_D = \frac{U_\infty D}{v} \quad (1)$$

$$\dot{m} = \rho u_m A$$

$$q = h\Delta T$$

$$q = \dot{m}\, C_p \Delta T$$

Appendix F: Engineering Calculations—Turbine

Airfoil selection

To maximize the efficiency of a turbine, it is important to maintain the optimal angle of attack over the blades. As shown in Figure F1, the angle of attack refers to the angle between the "relative wind", or the relative velocity of the incoming flow, and the Chord line of the airfoil.

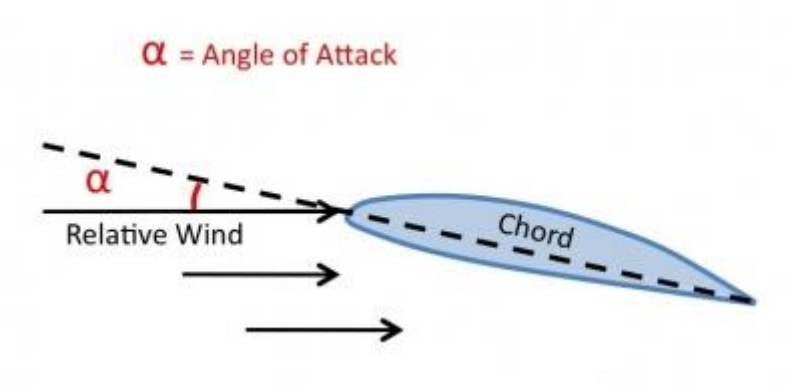

Figure F1: Airfoil Geometry [17]

The optimal angle of attack will provide the maximum ratio of lift and drag and depends on the airfoil profile selected. Thus, the first step in the design process was to select an airfoil profile. Dr. Acker suggested that a "cambered plate" type profile would be ideally suited in this application, due to the small scale and low Reynolds numbers. The website airfoiltools.com provides numerous cambered plate profiles as well as their best-suited Reynolds number ranges. To choose the initial profile, a very rough Reynolds number was estimated.

At this stage the team estimates that the model will have a diameter of about ten centimeters. The blades should occupy most of this space and will likely have a Chord length of around one centimeter. Unfortunately, it is difficult to estimate the mass flow rate in the final system. As a starting point, I researched the volumetric flow rate of a typical air mattress pump, which is about 21 cubic feet per minute (CFM), or approximately 0.01 cubic meters per second, and a leaf blower, which has a volumetric flow rate of about 200 CFM, or 0.1 cubic meters per second. [18, 19]. I estimate that our model will have a volumetric flow rate somewhere between these two. For this analysis, we will assume 0.05 m^3/s, but this is just a ballpark starting point which can easily be adjusted in the final MATLAB code.

Assuming this volumetric flow rate, and a turbine rotational velocity of about 5000 rpm (again this can be adjusted), we estimated the average Reynolds number of the center of the airfoil to be approximately 8000. The calculation is detailed below.

$$\vec{V} = \vec{W} + \vec{U}$$

Where V = absolute (incoming) velocity, W = relative velocity, and U = blade velocity. W is the important velocity here, as it is the velocity that the blade experiences. It is important to note that this expression is a vector sum.

$$\dot{\forall} = V * A; V = \frac{\dot{\forall}}{A}$$

Where $\dot{\forall}$ = volumetric flow rate and A = cross sectional area.

$$A = \frac{\pi}{4}(D)^2 = \frac{\pi}{4}(0.1m)^2$$

Where D = casing diameter.

$$V = \frac{0.05\ m^3/s}{\frac{\pi}{4}(0.1m)^2} = 6.36\frac{m}{s} \approx 6.5\ m/s$$

$$U_{avg} = r_{avg}\omega = (0.025m)\left(5000\frac{rev}{\min}\right)\left(2\pi\frac{rad}{rev}\right) = 13.1\frac{m}{s} \approx 13\ m/s$$

r_{avg} = midpoint radius, ω = angular velocity

$$W = \sqrt{V^2 + U^2} = \sqrt{\left(6.5\frac{m}{s}\right)^2 + \left(13\frac{m}{s}\right)^2} = 14.53\frac{m}{s} \approx 14.5\frac{m}{s}$$

$$Re = \frac{\rho V c}{\mu}$$

Re = Reynolds Number, ρ= fluid density, c= chord length, μ = dynamic viscosity.

$$At\ 7000\ ft\ (\sim 2000\ m), \frac{\rho}{\rho_{SL}} = 0.8217\ \Rightarrow\ \rho \approx 1.007\frac{kg}{m^3}$$

$$Re = \frac{\left(1.007\frac{kg}{m^3}\right)\left(14.5\frac{m}{s}\right)(0.01m)}{(1.81E-5\frac{Ns}{m^2})} \approx 8067$$

Most standard airfoils operate at significantly higher Reynolds numbers. Dr. Acker suggested that airfoil design is not as critical at low Reynolds numbers, so for this analysis we selected a standard cambered plate airfoil at the lowest Reynolds number range, which is 50,000. The selected airfoil is a cp-140-050gn cambered plate, shown below in Figure F2. This airfoil has an optimal angle of attack of 13.25 degrees [20].

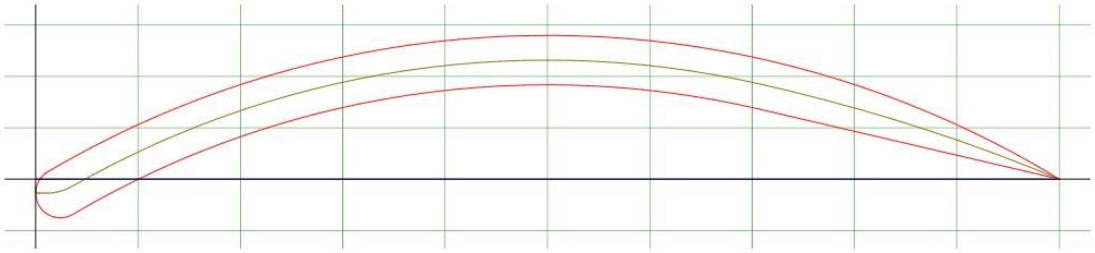

Figure F2: Selected Airfoil Profile [20]

Angle of Attack Calculation

As noted previously, the goal is to maintain this angle of attack over the entire length of the blade. As shown in Figure F1, this is the angle between the relative wind and the Chord line of the airfoil. *Fundamentals of Gas Turbines* provides an excellent diagram illustrating the geometry of the flow entering a rotor stage, illustrated in Figure F3. In this example, V_1 is the incoming axial flow, W_1 is the

relative velocity, and β is the angle of the relative velocity with respect to the axial direction. In this example, it is assumed that the axial velocity is one dimensional in the axial direction, and the relative velocity enters the rotors at the Chord line angle, meaning the angle of attack is zero. This type of diagram is known as a velocity triangle.

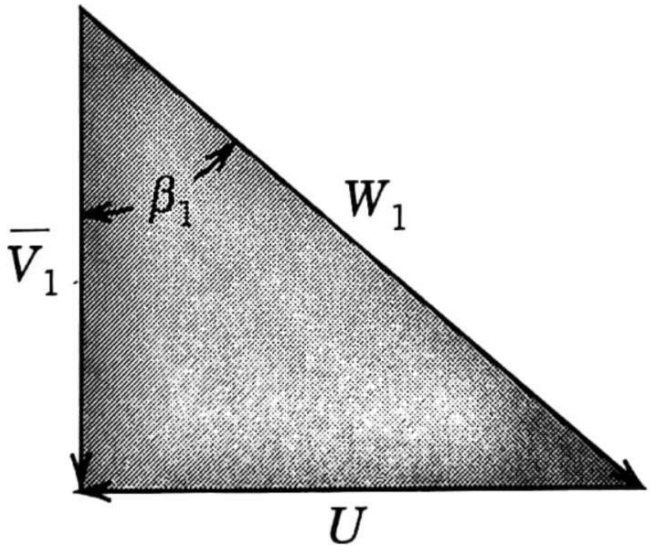

disc

Figure F3: Velocity Triangle [21]

This example can be expanded to demonstrate a flow with a positive angle attack. Figure F4 illustrates this theory using the selected airfoil profile. In the figure, γ is the angle between the chord line and the axial direction, which will be defined as the pitch angle, and α is the angle between the chord line and the relative wind, which is the angle of attack.

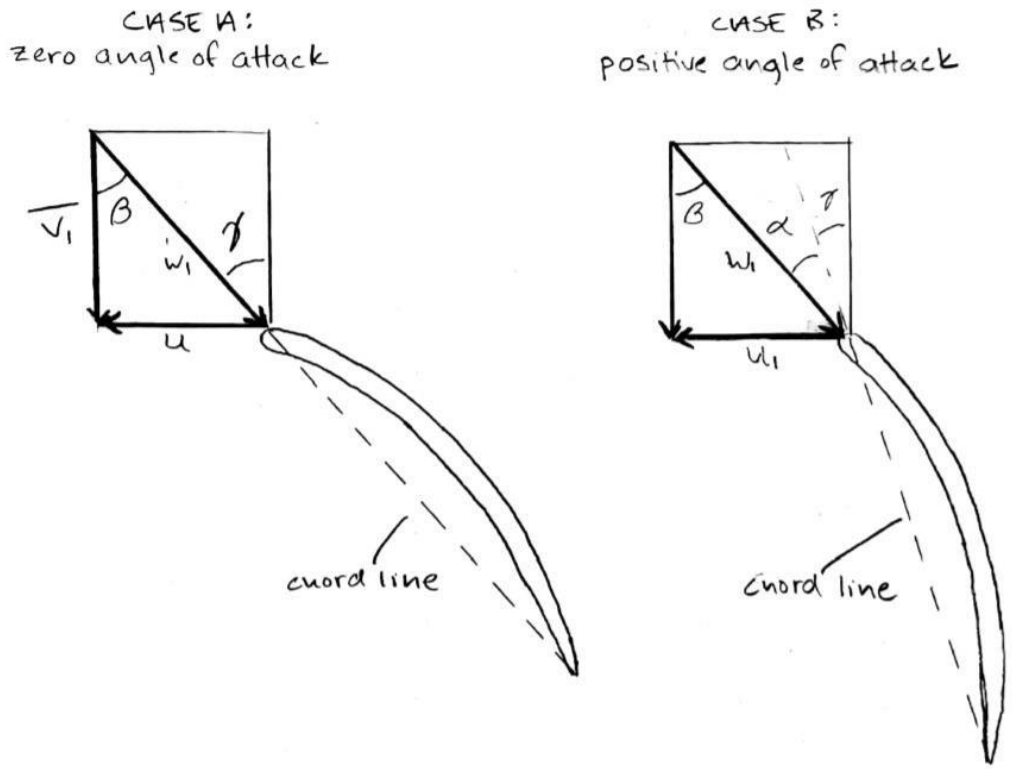

Figure F4: Airfoils with Velocity Triangles

Case A is the same as in Figure F3, where the flow enters at the same angle as the chord line, and the angle of attack is zero. In Case B, the incoming velocity is identical to Case A. This time, however, the blade is oriented differently to create a positive angle of attack. By inspection, the angles β and $\alpha + \gamma$ constitute alternate interior angles, meaning $\beta = \alpha + \gamma$.

However, as noted previously, the blade velocity U will vary depending on radial location along the blade. As a result, β will also change. To maintain a constant angle of attack, the pitch angle γ must be continuously varied radially along the blade profile. This angle can be calculated at each location using the equation $\gamma = \beta - \alpha$. Since this value continuously changes, the best way to calculate parameter is by creating a MATLAB script which discretizes the blade profile into finite elements and calculates γ for each element.

MATLAB Program

The MATLAB script for this analysis prompts a user to input the volumetric flow rate in CFM, angular velocity in RPM, casing diameter in centimeters (cm), and desired angle of attack in degrees. It also asks the user how many elements they would like the blade to be discretized into. Using this information, the program makes necessary unit conversions, then calculates axial velocity using the method detailed in the Airfoil Selection section. Next, it calculates blade velocity at each point along the blade based on the radial location of each blade element. It then calculates the relative flow angle and the necessary pitch angle to maintain the desired angle of attack at each location. The final output is a plot which displays pitch angle in degrees vs. the radial location in meters. Figure F5 below shows an example output using a flow rate of 100 CFM, an angular velocity of 5000 RPM, a casing diameter of 10 cm, an angle of attack of 13.25 degrees, and 100 blade elements.

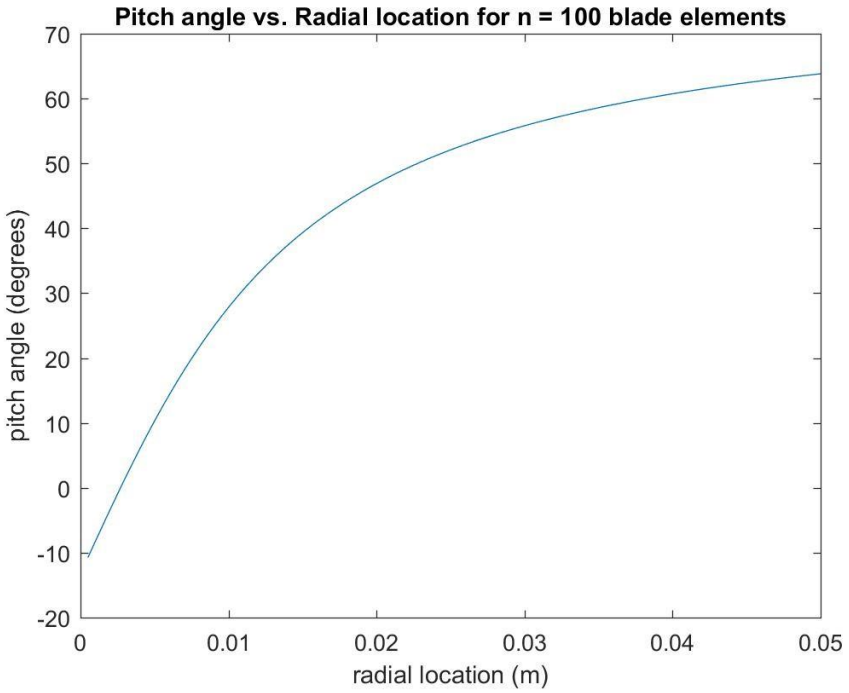

Figure F5: Pitch Angle vs. Radial Location

This code makes several assumptions. First, it assumes the incoming axial velocity is one dimensional and enters parallel to the axial direction. It also assumes that each blade occupies half the inner diameter (ignoring the shaft at the center). The script is presented below in its entirety

```
% Programmer: Jacob Barker
% Date: 03/09/18
%%%%%%%%%%%%%%%%%%%%%%%%%%%%%%%%%%%%%%%%%%%%%%%%%%%%%%%%%%%%%%%%%%%%%%%%%%%%%%%

clear; clc; close all;

%prompt user for volumetric flow rate
Vdot1 = input('Enter volumetric flow rate (CFM): ');

%prompt user for angular velocity
RPM = input('Enter angular velocity (RPM): ');

%prompt user for desired number of blade elements n =
input('Enter desired number of blade elements: n = ');

%prompt user for desired angle of attack
alpha = input('Enter angle of attack (degrees): ');

%Prompt user for outer diameter
d1 = input('Enter housing diameter (cm): d = ');

%convert units
Vdot = Vdot1*(1/60)*(12^3)*(2.54^3)*(100^(-3)); %m^3/s

omega = RPM*2*pi/60; %rad/s
  d = d1/100;
%m
  r = d/2;
%m
%ignores shaft diameter, assumes blades occupy entire cross section

%distance between blade element "nodes" dx
= r/(n-1);

%blade element "node" locations. "Off the edge" configuration as
%blade tip angle important. Starts at dx as there is no blade velocity
%at zero (shaft location) x
= dx:dx:r;

%caclulate axial velocity Va
= Vdot/(pi/4*d^2);

%Create blank vectors for U, W, beta, gamma to be populated in for loop
```

```
U = zeros(1,length(x)); W
= zeros(1,length(x)); beta
= zeros(1,length(x));
gamma = zeros(1,length(x));

for i = 1:length(x)
    U(i)=x(i)*omega;

    W(i)=sqrt((x(i)^2)+Va^2);

    beta(i)=radtodeg(atan(U(i)/Va));

    gamma(i)=beta(i)-alpha;
     end  plot(x,gamma) xlabel('radial location (m)') ylabel('pitch
angle (degrees)') title(['Pitch angle vs. Radial location for n = '
num2str(n) ' blade elements'])
```

Appendix G: Updated Bill of Materials

Table G1 shows the current Bill of Materials for the project. The items highlighted in yellow indicate that they were purchased by the previous capstone team, and thus are not part of our $500 allotted budget.

Table G1: Updated Bill of Materials

Item	Quantity	Cost per unit	Subtotal	Manufacturer	Item #	Vendor	Hyperlink
Acrylic Tubing	23 7/8 in	$17.99	$17.99	estreetplastics	ET0450042524	estreetplastics	https://goo.gl/rmKMEm
3D Printed Compressor Blades	255 g	$0.10	$25.50	MakerBot	N/A	NAU Cline Library	n/a
3D Printed Compressor Stator Blades	292 g	$0.10	$29.20	MakerBot	N/A	NAU Cline Library	n/a
3D Printed Turbine Blades	152 g	$0.10	$15.20	MakerBot	N/A	NAU Cline Library	n/a
3D Printed Turbine Stator Blades	213 g	$0.10	$21.30	MakerBot	N/A	NAU Cline Library	n/a
3D Printed Combustion Chamber	208 g	$0.10	$20.80	MakerBot	N/A	NAU Cline Library	n/a
3D Printed Test Fitting #1	77.58 g	$0.10	$7.76	MakerBot	N/A	NAU Cline Library	n/a
3D Printed Test Fitting #2	64.28 g	$0.10	$6.43	MakerBot	N/A	NAU Cline Library	n/a
Aluminum Shaft	2 ft	$5.62	$5.62	MetalsDepot	R3516	Metals Depot	https://goo.gl/CezFTP
Ceramic 608 Bearings	2	$3.33	$6.66	VXB	608-2RS-DRY	VXB	https://goo.gl/zPNP8M
Air compressor with tank	1	$89.00	$89.00	Porter Cable	C2002	CPO Commerce	https://goo.gl/KRQu8p
Band Heater	1	$28.50	$28.50	Tempco	NHL00100	Grainger	https://goo.gl/WnqnU8
K Type Thermocouple Wire	25 ft	$0.86	$21.50	TIP Industries	TIPWRK004	TIP Industries	https://goo.gl/AETaH8
Thermocouple Connectors	4	$2.30	$9.20	Omega	OST-U-M	Omega	https://goo.gl/mftfh2
Thermocouple DAQ	1	$107.00	$107.00	National Instruments	USB-TC01	National Instruments	https://goo.gl/U5soAU
1/4 in. x 1/4 in. MIP Brass Compression Adapter	2	$4.40	$8.80	Everbilt	801079	Home Depot	https://goo.gl/z6qf8e
Brass Pipe Coupling 1/4 in. FIP	2	$4.16	$8.32	Everbilt	801889	Home Depot	https://goo.gl/VR7m58
Brass Compression Tee 1/4 in	2	$7.51	$15.02	Everbilt	800849	Home Depot	https://goo.gl/Nh2w24
1/4 in. Compression Angle Needle Valve	4	$8.80	$35.20	Everbilt	800539	Home Depot	https://goo.gl/NpVaUW
1/4 in. O.D. x 0.170 in. I.D. x 10 ft. PVC Clear Vinyl Tube	1	$2.82	$2.82	Everbilt	701906	Home Depot	https://goo.gl/pECLr4
Pressure Transducer	2	$49.00	$98.00	Transducers Direct	TDH30BG025003B004	Transducers Direct	https://goo.gl/ZAUC21
Pressure Transducer DAQ	1	$250.00	$250.00	National Instruments	USB-6009	National Instruments	https://goo.gl/xaw9sP
Cart	1	$37.99	$37.00	US General	5107	Harbor Freight	https://goo.gl/gR9cP3
		Total:	**$866.82**				
		Our Cost:	$401.32				